三峡大学
CHINA THREE GORGES UNIVERSITY

Chiral Magnetic Effects and Magnetic Field Features in Relativistic Heavy-Ion Collisions

1. Introductions
2. The Magnetic Fields in Realtivistic HIC
3. Chiral Electromagnetic Current in Relativistic HIC
4. Charge Separation in Relativistic HIC
5. Magnetic Field Induced Polarization Difference between Λ and $\bar{\Lambda}$

Sheng-Qin Feng（冯笙琴） China Three Gorges University (CTGU 三峡大学)

Collab. with: X. Ai， Y. Guo, J. Liao, Y. -J. Mo, D. She and Y. Zhong

2019弦论、场论与宇宙学相专题研讨会，宜昌， November 22-25, 2019

三峡大学
CHINA THREE GORGES UNIVERSITY

1. Introduction

D. Kharzeev, L. D. Mclerran, H. J. Warringa, NPA 803, 227 (2008)

2019弦论、场论与宇宙学相专题研讨会，宜昌，November 22-25, 2019

三峡大学
CHINA THREE GORGES UNIVERSITY

Strong

Strong matter produced
in heavy ion collisions

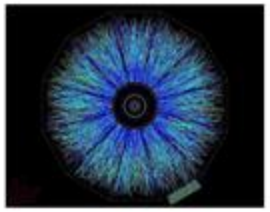

Topological charge changing transitions

induce difference between number of left- and right-handed fermions

Parity to be violated locally in microscopic domains in QCD at finite temperature

ElectroWeak Matter

Electroweak matter produced
in the early universe

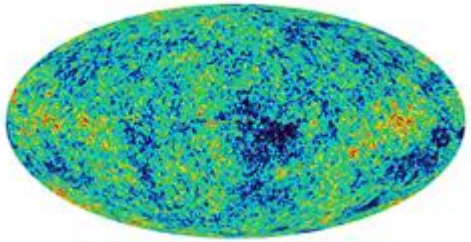

Topological charge changing transitions

induce nonzero baryon + lepton number

Parity to be violated globally of weak interactions of the standard model

At high temperatures these transitions are unsuppressed (Sphalerons)
Manton ('83), Manton and Klinkhamer ('84), Mclerran and Shaposhnikov ('85)

How to observe topological charge changing transitions in hot quark matter?

Kharzeev, Mclerran, Warringa, ('08)

An asymmetry between matter and antimatter is observed
Kuzmin, Shaposhnikov ('85)

Instantons and Sphaleron

$$Q_w = \frac{g^2}{8\pi^2}\int d^4x\, \vec{E}_a \cdot \vec{B}_a = 0, \pm 1, \pm 2, \ldots.$$

Stable under smooth deformations
Change topological charge vacuum

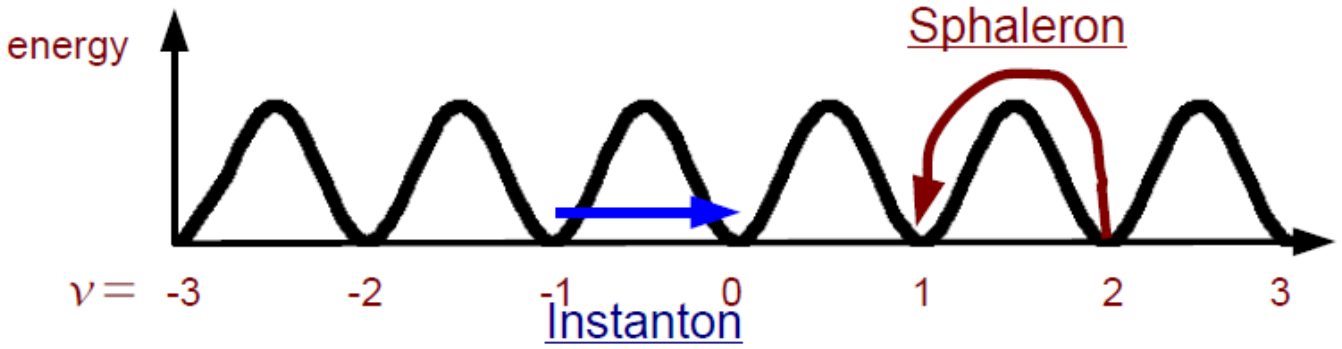

Instantons: Configuration with finite action. **Tunneling through barrier**

Suppression of rate at T=0, 't Hooft ('76), Pisarski and Yaffe ('80)

Sphaleron: Configuration with finite energy. Go over barrier.

Only possible at finite temperature, rate not suppressed, look for it in QGP!

Manton ('83), Manton and Klinkhamer ('84), McLerran, Mottola and Shaposhnikov ('88)

$$\frac{d N_t^{\pm}}{d^3x\, d\, t} \sim 385\, \alpha_S^5\, T^4$$

Bödeker, Moore and Rummukainen ('00), several transitions per fm^{-3} per fm/c

The Chiral Magnetic Effect (CME)

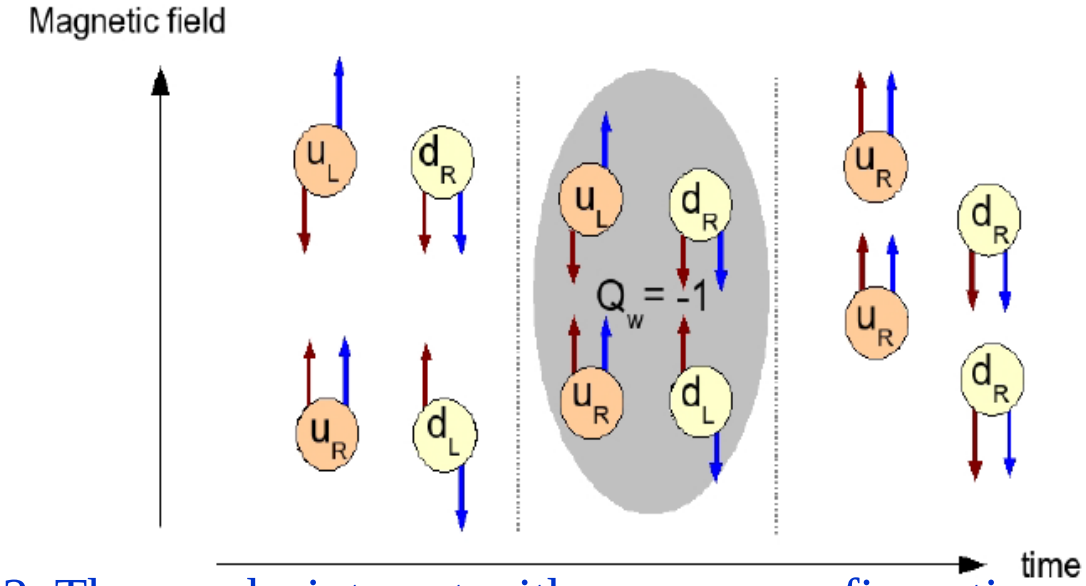

1. Due to very large magnetic field, the up and down quarks in the lowest landau level and can only move along the direction of the magnetic field. Initially there are as many left-handed as right-handed quarks.

2. The quarks interact with a gauge configuration with non-zero Q_w. Assuming $Q_w = -1$, this will convert a left-handed up/down quark into a right-handed up/down quark by reversing the direction of momentum.

3. The right-handed up quarks will move upwards, the right-handed down quarks will move downwards. A charge of q = 2e will be created between two sides of a plane perpendicular the magnetic fields

In finite volume this causes separation of positive from negative charge

In presence of magnetic field，this induces a chiral electromagnetic current

D. Kharzeev, L. D. Mclerran, H. J. Warringa, NPA 803, 227 (2008)

The Chiral Magnetic Effect

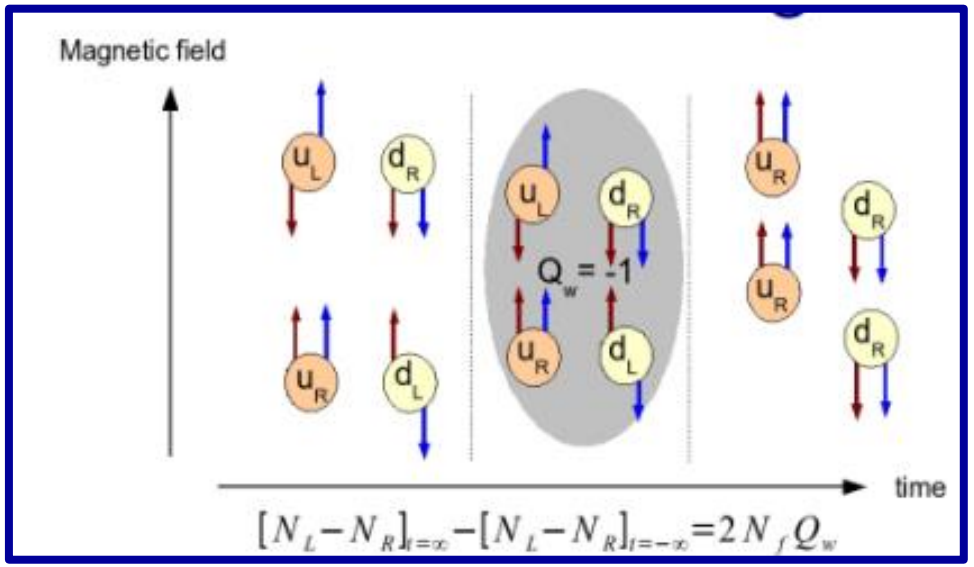

Charge difference:

$$Q = 2Q_w \sum_f |q_f|$$

Same sign for antiparticles!

Toplogical charge changing transitions induces chirality

In finite volume this causes separation of positive from negative charge

Reasonable polarization of quarks requires: $eB \sim \frac{1}{\rho^2} \sim \alpha_s^2 T^2 \sim 10^3 - 10^4 \text{ MeV}^2$

D. Kharzeev, L. D. Mclerran, H. J. Warringa, NPA 803, 227 (2008)

三峡大学
CHINA THREE GORGES UNIVERSITY

2. Magnetic Field in HIC

2019弦论、场论与宇宙学相专题研讨会，宜昌，November 22-25, 2019

Consider the thickness of the Lorentz contraction of the collision nuclear in the Z directions

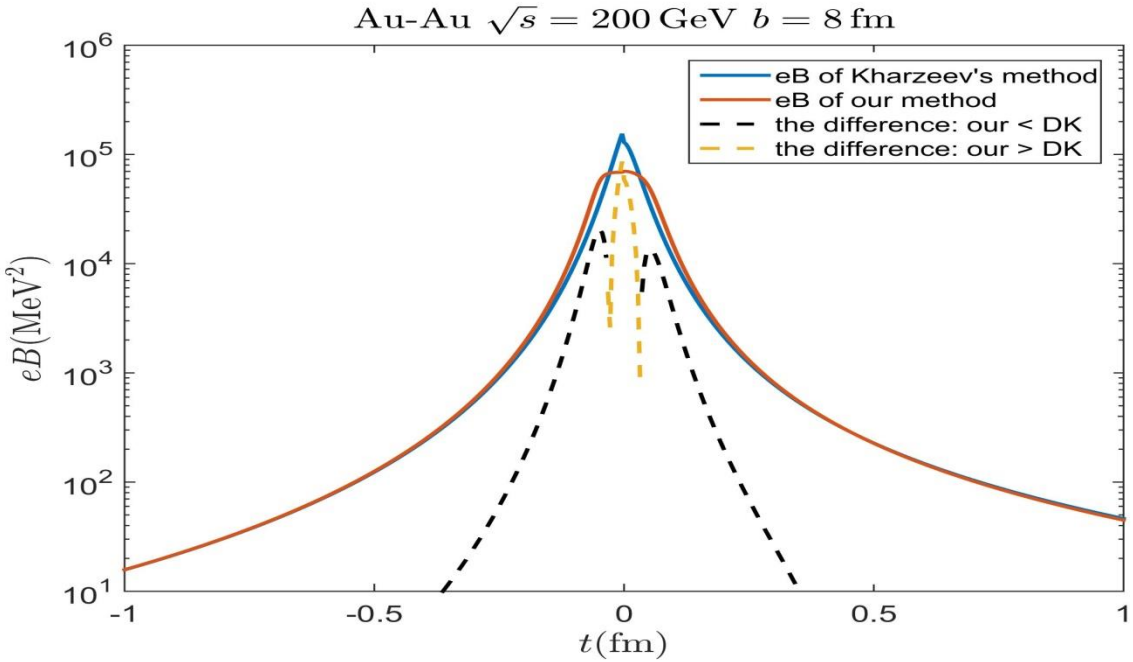

KMW's model --**pancake approximation(z → 0), we consider the thickness in the *z* direction**

RHIC@BNL

$$eB(\tau = 0.2\,\mathrm{fm}) = 10^3 \sim 10^4\ \mathrm{MeV}^2 \sim 10^{17}\,\mathrm{G}$$

Reasonable polarization of quarks requires: $eB \sim 1/\rho^2 \sim 10^3 - 10^4\,\mathrm{MeV}^2$

Y. -J. Mo, S. -Q. Feng and Y. -F. Shi, Phys. Rev. C 024901 (2013);
Y. Zhong, C.-B. Yang, X. Cai and S. -Q. Feng , Adv. High Energy Phys. 2014 (2014) 193039

D. Kharzeev, L. D. Mclerran, H. J. Warringa, NPA 803, 227 (2008)

Comparison of Magnetic fields of RHIC with LHC

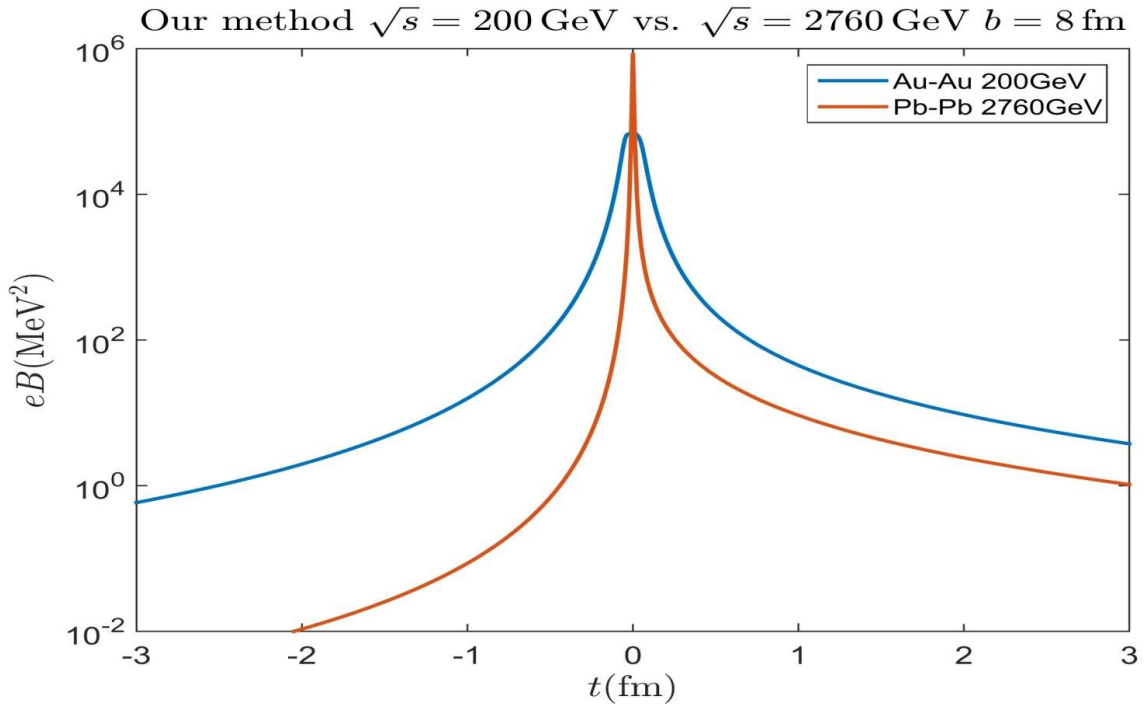

At LHC, magnetic fields falls off rapidly with time than that at RHIC, Chiral Magnetic Effect Is early time dynamics

$$eB\,(t = 0.2\mathrm{fm}) = 10^3 \sim 10^4\,\mathrm{MeV}^2 \sim 10^{17}\,\mathrm{G} \quad (200\mathrm{GeV})$$

$$eB\,(t = 0.2\mathrm{fm}) = 10^2 \sim 10^3\,\mathrm{MeV}^2 \sim 10^{16}\,\mathrm{G} \quad (2760\mathrm{GeV})$$

Low energy quarks which are produced in early stages will be polarized in the direction perpendicular to reaction plane

Y. -J. Mo, S. -Q. Feng and Y. -F. Shi, Phys. Rev. C 024901 (2013);
Y. Zhong, C. -B. Yang, X. Cai and S. -Q. Feng , Adv. High Energy Phys. 2014 (2014) 193039

Magnetic field distributes with space and time

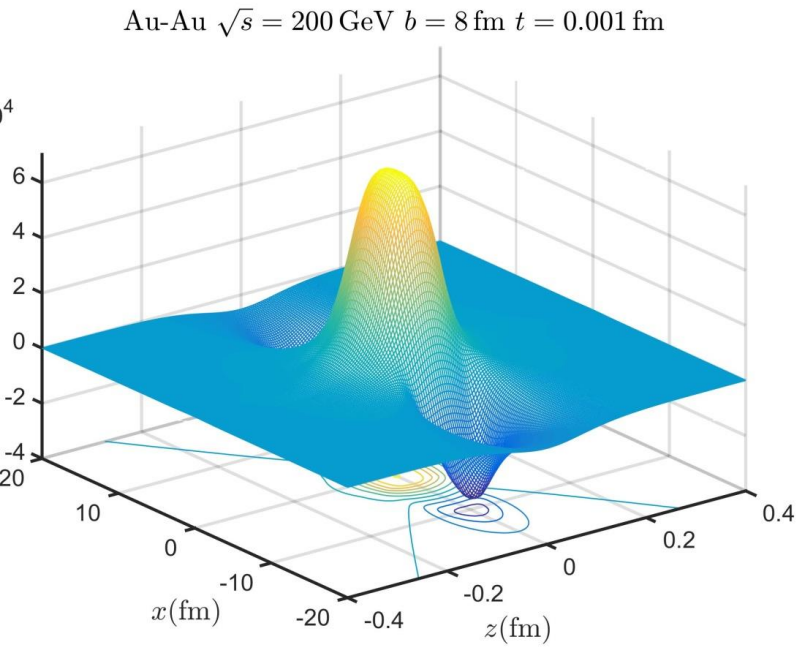

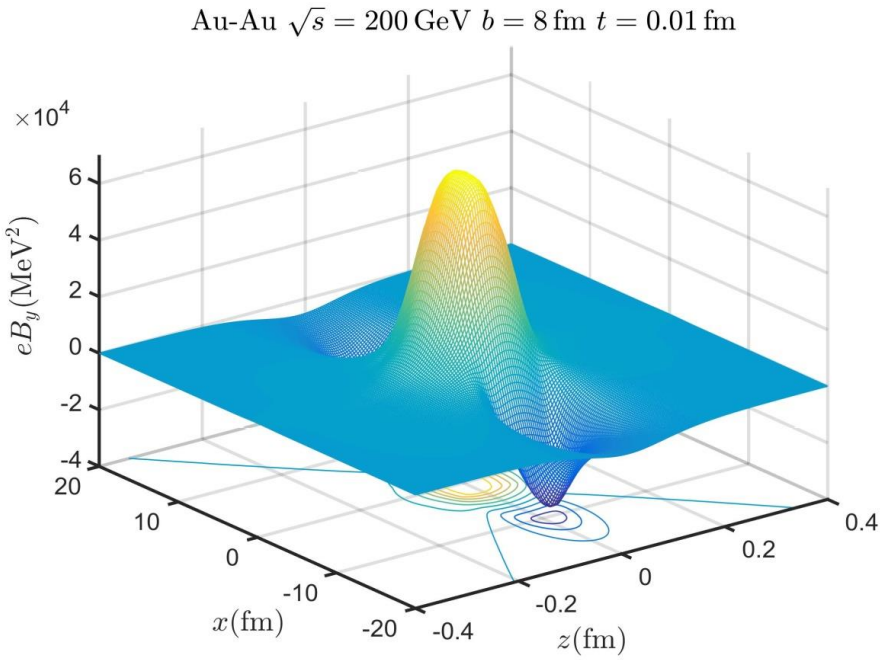

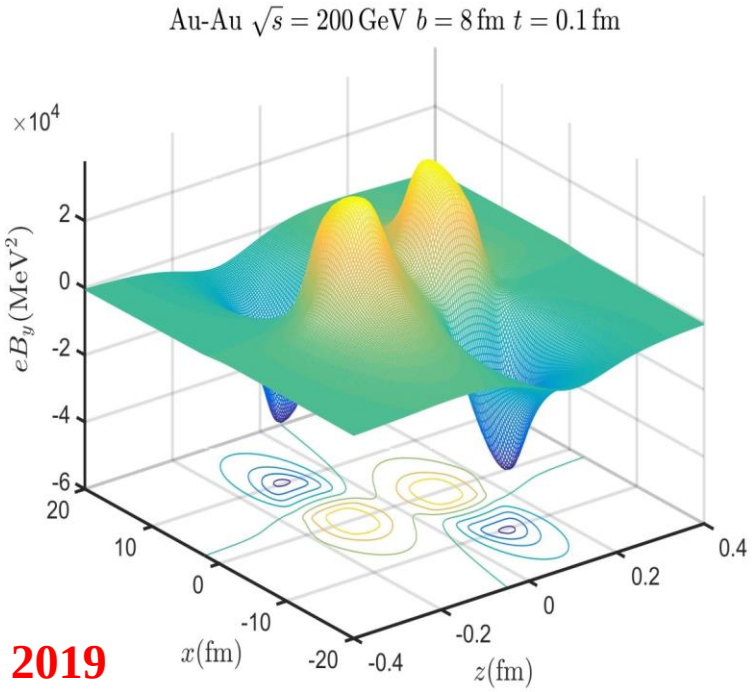

Y. Zhong, C.-B. Yang, X. Cai and S. -Q. Feng , Adv. High Energy Phys. 2014 (2014) 193039

Magnetic fields change with collision energy at early time

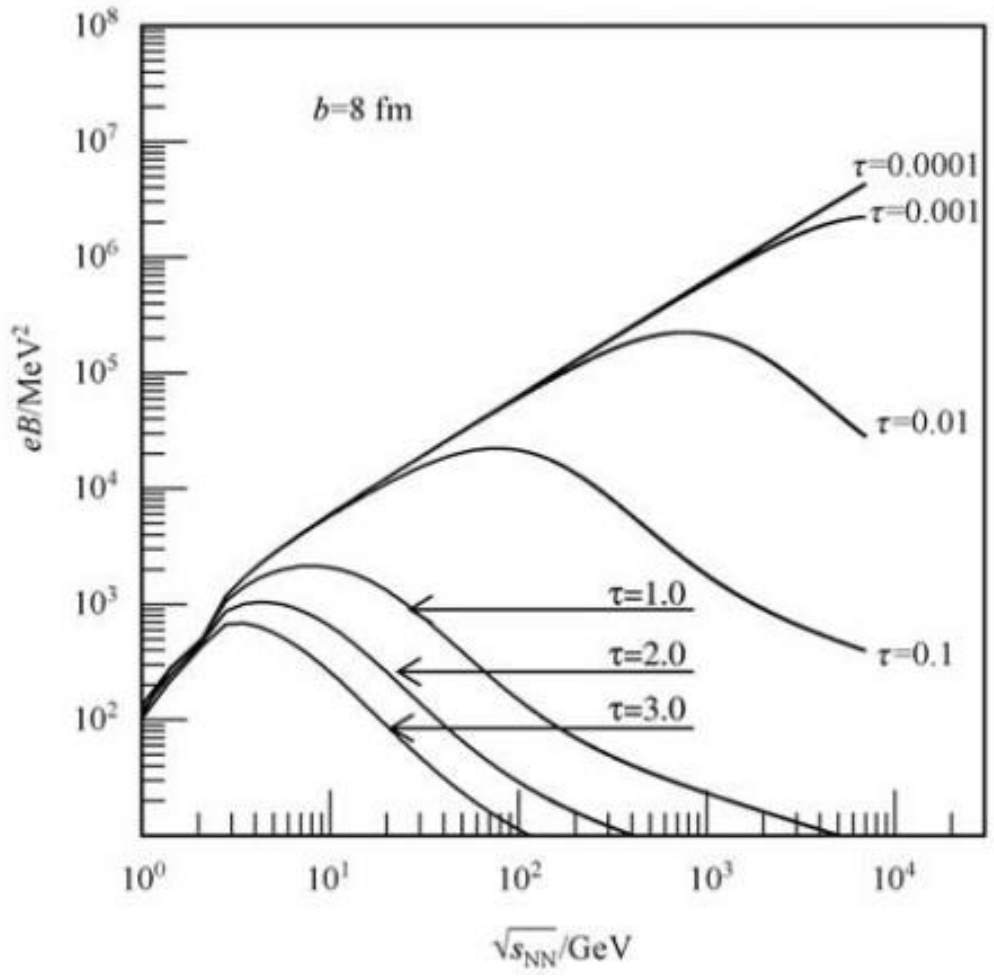

Y. Zhong, C.-B. Yang, X. Cai and S. -Q. Feng , Adv. High Energy Phys. 2014 (2014) 193039

Consider the response of QGP in relativistic heavy-ion collisions

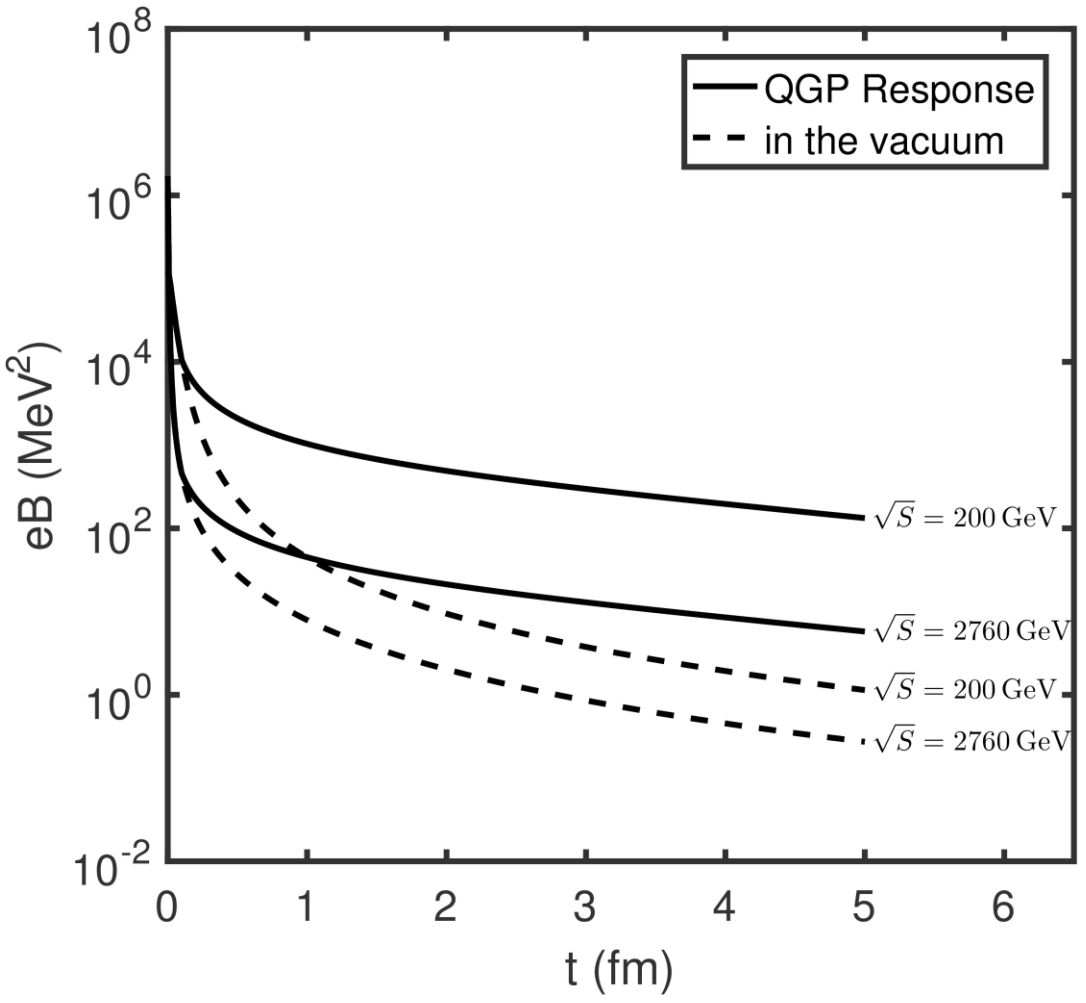

Coupled Maxwell +hydro: W. T. Deng, and X. G. Huang, Phys. Rev. C 85, 044907 (2012).

D. She, S. -Q. Feng, et al., European Physical Journal A 54: 48 (2018)

Magnetic fields from Beam Energy Scanning (BES)

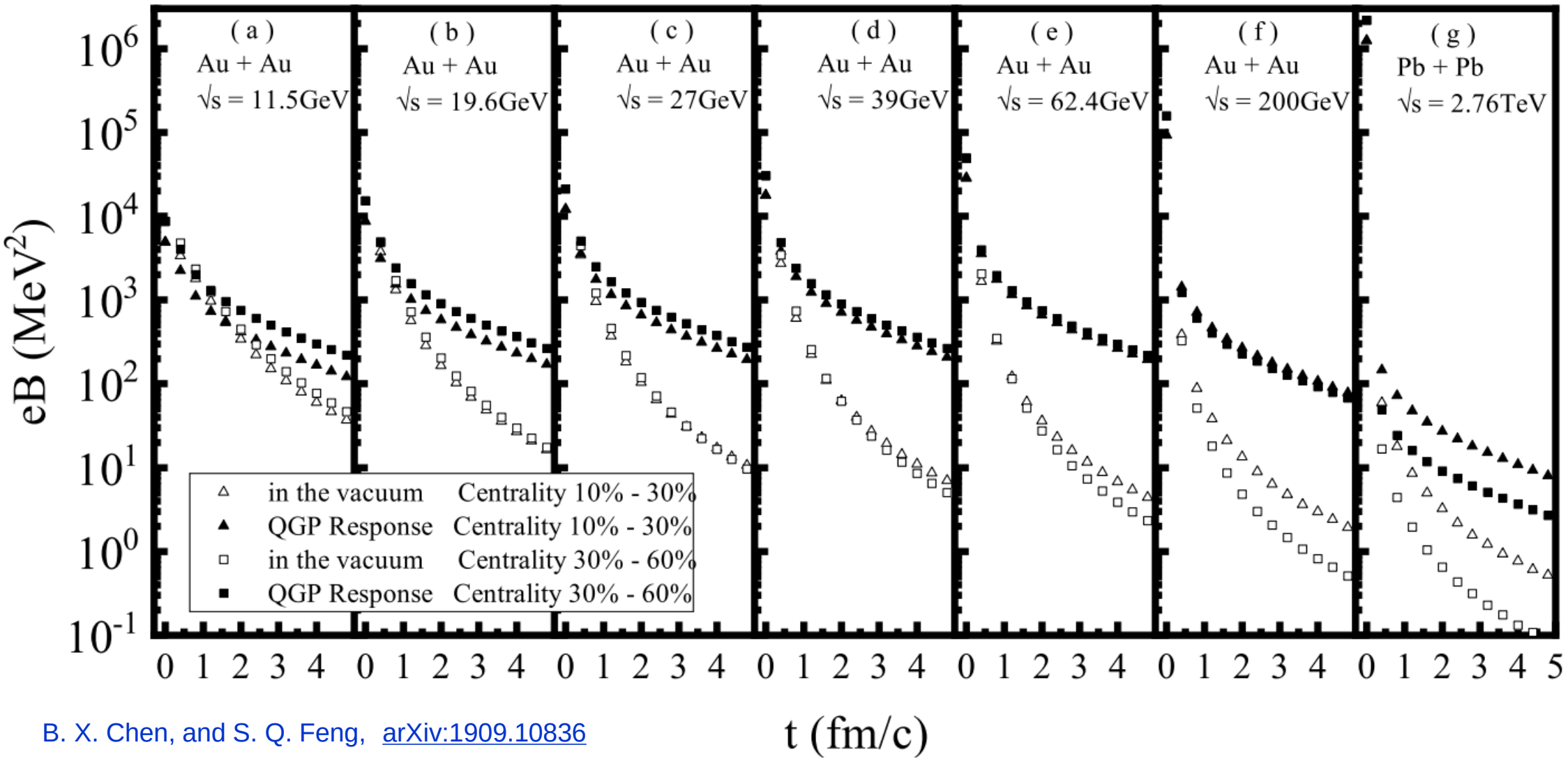

B. X. Chen, and S. Q. Feng, arXiv:1909.10836

Comparison with other group calculation results

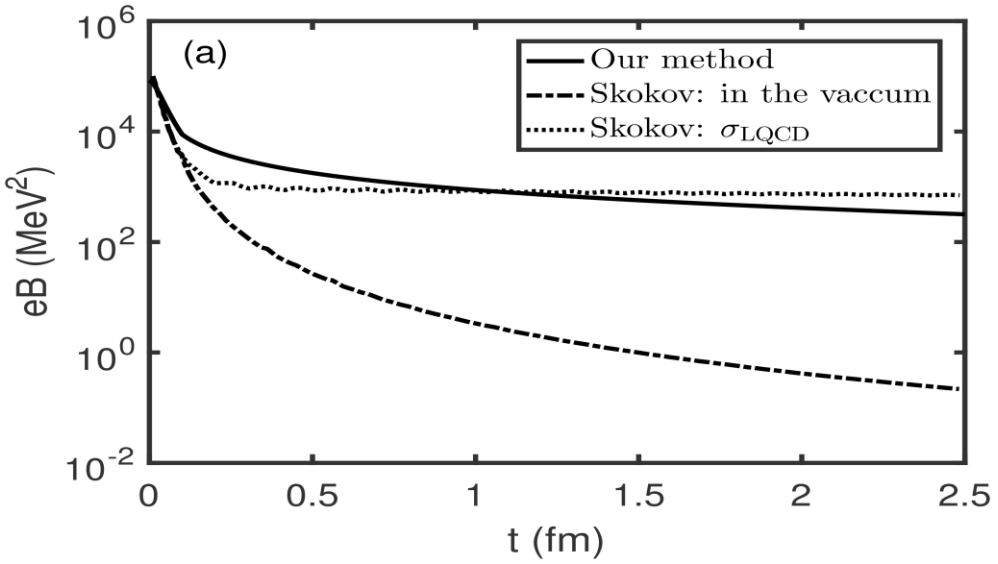

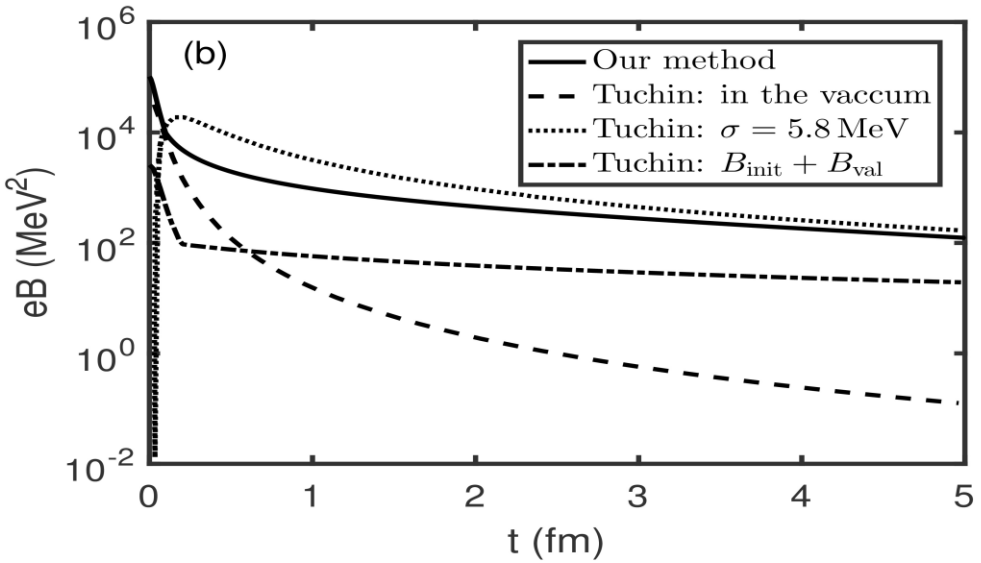

1. L. McLerran, V. Skokov, Nucl. Phys. A929, 184 (2014).

2. K. Tuchin, Phys. Rev. C 93, 014905 (2016).

D. She, S. -Q. Feng, European Physical Journal A 54 : 48 (2018)

三峡大学
CHINA THREE GORGES UNIVERSITY

3. Chiral Electromagnetic Current

Based on: D. She, S. -Q. Feng, European Physical Journal A 54:48 (2018)

Chiral Magnetic Conductivity (CMC)

The induced vector current can be calculated using the Kubo formula. This formula is provided by using first order in the time-dependent perturbation:

$$< j^{\mu}(x) >= \int d^4x' \Pi_R^{\mu\nu}(x,x') A_v(x')$$

Where $j^{\mu}(x) = e\bar{\psi}(x)\gamma^{\mu}\psi(x)$ **, and the retarded response function is given by**

$$\Pi_{\mathrm{R}}^{\mu\nu}(x,x') = i\langle[j^{\mu}(x), j^{\nu}(x')]\rangle\theta(t-t').$$

Select vector field: $A_x = A_z = 0, A = A_y$

Then: $B_z = \partial_x A_y(x)$

The induced vector current in the magnetic field direction:

$$\langle j_z(x)\rangle = \sigma_{\chi}(p)\tilde{B}_z(p)e^{-ipx} \qquad \sigma_{\chi}(p) = \frac{1}{ip^1}\tilde{\Pi}_R^{23}(p) = \frac{1}{2ip^i}\tilde{\Pi}_R^{jk}(p)\varepsilon^{ijk}$$

Chiral magnetic conductivity(CMC):

$$\sigma_{\chi}(p) = \frac{1}{ip^i}G_R^i(p) \qquad G_R^i(p) = \frac{1}{2}\varepsilon^{ijk}\tilde{\Pi}_R^{jk}(p)$$

Retarded Correlator

Retarded correlator can be given by Euclidean correlator:

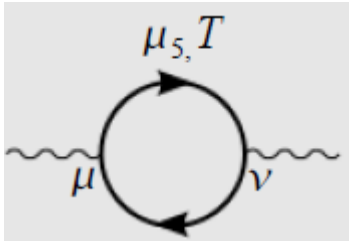

$$G_{\mathrm{R}}^{i}(p_0, \boldsymbol{p}) = G_{\mathrm{E}}^{i}(\omega_n, \boldsymbol{p})|_{i\omega_n \to p_0 + i\epsilon}$$

At very high temperatures，Euclidean correlator:

$$G_{\mathrm{E}}^{i}(P) = \frac{e^2}{2\beta} \sum_{\tilde{\omega}_m} \int \frac{d^3q}{(2\pi)^3} \epsilon^{ijk}\, \mathrm{tr}[\gamma^k S(Q) \gamma^j S(P+Q)]$$

The bare fermion propagator as a function of Euclidean momentum Q in the presence of a chiral chemical potential

$$S(Q) = \frac{1}{i\gamma^0(\tilde{\omega}_m - i\mu - i\mu_5\gamma^5) - \boldsymbol{\gamma}\cdot\boldsymbol{q}},$$

From fermion propagator and chirality projection operators, the integrand function can be written:

$$\boldsymbol{G_R^i(p) = \frac{ie^2}{16\pi^2}\frac{p^i}{p}\frac{p^2 - p_0^2}{p^2}\int_0^\infty dq f(q) \sum_{t=\pm}(2q + tp_0) \times log[\frac{(p_0 + i\varepsilon + tq)^2 - (q+p)^2}{(p_0 + i\varepsilon + tq)^2 - (q-p)^2}]}$$

$$f(q) \equiv \sum_{s=\pm} s[\tilde{n}(q - \mu_s) - \tilde{n}(q + \mu_s)]$$

Real and Imaginary Part of CMC

At zero temperature:

$$\sigma_\chi''(\omega) = \frac{e^2}{3\pi}\omega\delta(\omega)\mu_5 - \frac{e^2\omega^2}{96\pi}\sum_{s,t=\pm} st\delta(\omega/2 + t\mu_s)$$

For large temperature:

$$\sigma_\chi''(\omega) = \frac{e^2}{3\pi}\omega\delta(\omega)\mu_5 + \frac{e^2\omega|\omega|}{24\pi T^2}\tilde{n}(|\omega|/2)^3 \times [e^{|\omega|/T} - e^{|\omega|/(2T)}]\mu_5.$$

By **Kramers-Kroning realtion:**

$$\sigma_\chi'(\omega) = \frac{1}{\pi}\mathcal{P}\int_{-\infty}^{\infty} dq_0 \frac{\sigma_\chi''(q_0)}{q_0 - \omega},$$

$$\sigma_\chi''(\omega) = -\frac{1}{\pi}\mathcal{P}\int_{-\infty}^{\infty} dq_0 \frac{\sigma_\chi'(q_0)}{q_0 - \omega}.$$

Frequency and momentum dependence of the chiral magnetic conductivity

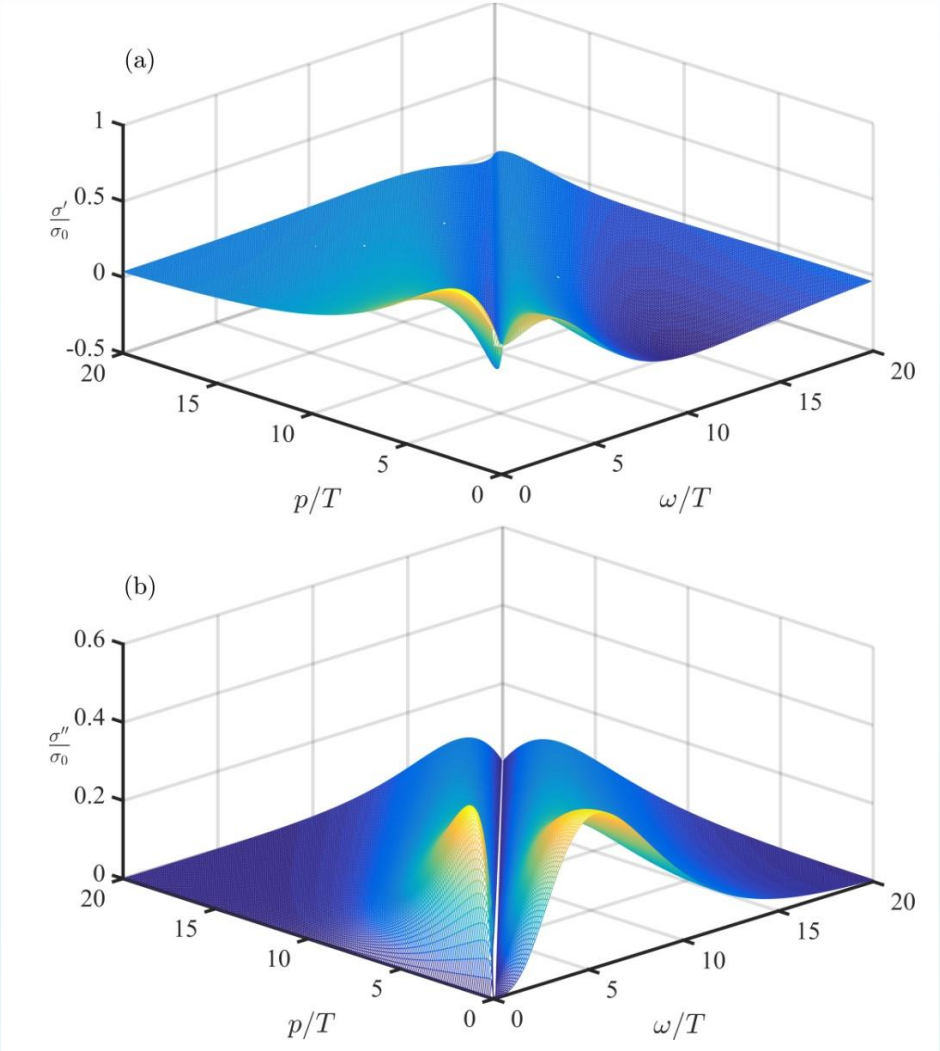

$\mu = 10\text{MeV},\ \mu_5 = 1\text{MeV},\ T = 200\text{MeV}$

D. She, S. -Q. Feng, European Physical Journal A 54:48 (2018)

Chiral Electromagnetic Current (CEC) in different temperatures

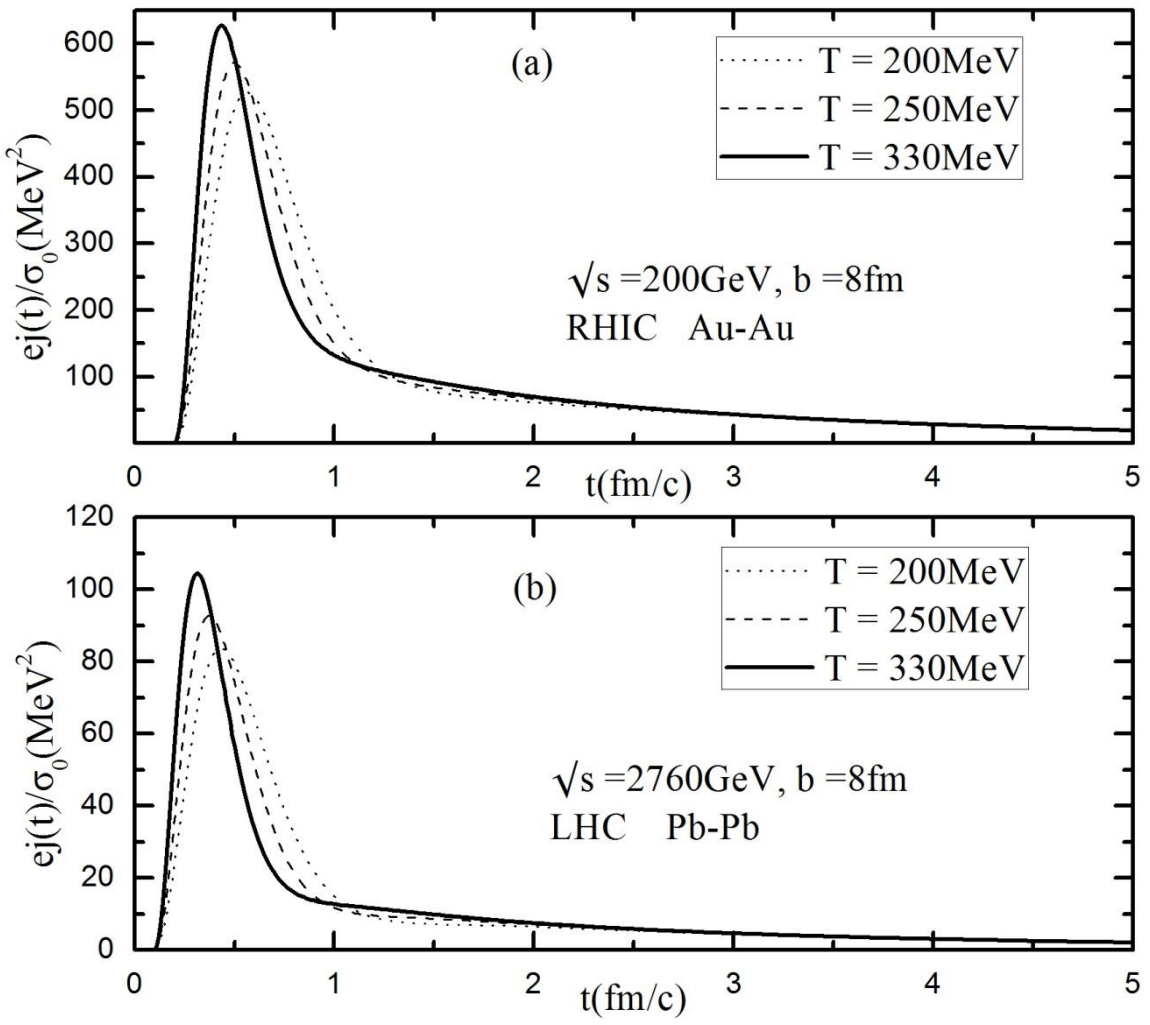

$$j(t) = \int_0^\infty \frac{d\omega}{\pi}[\sigma'(\omega)\cos(\omega t) + \sigma''(\omega)\sin(\omega t)]\tilde{B}(\omega).$$

$$\tilde{B}(\omega) = \int_{-\infty}^{\infty} dt e^{i\omega t} B(t).$$

D. She, S. -Q. Feng, European Physical Journal A 54:48 (2018)

Comparison by QGP response with in the vacuum

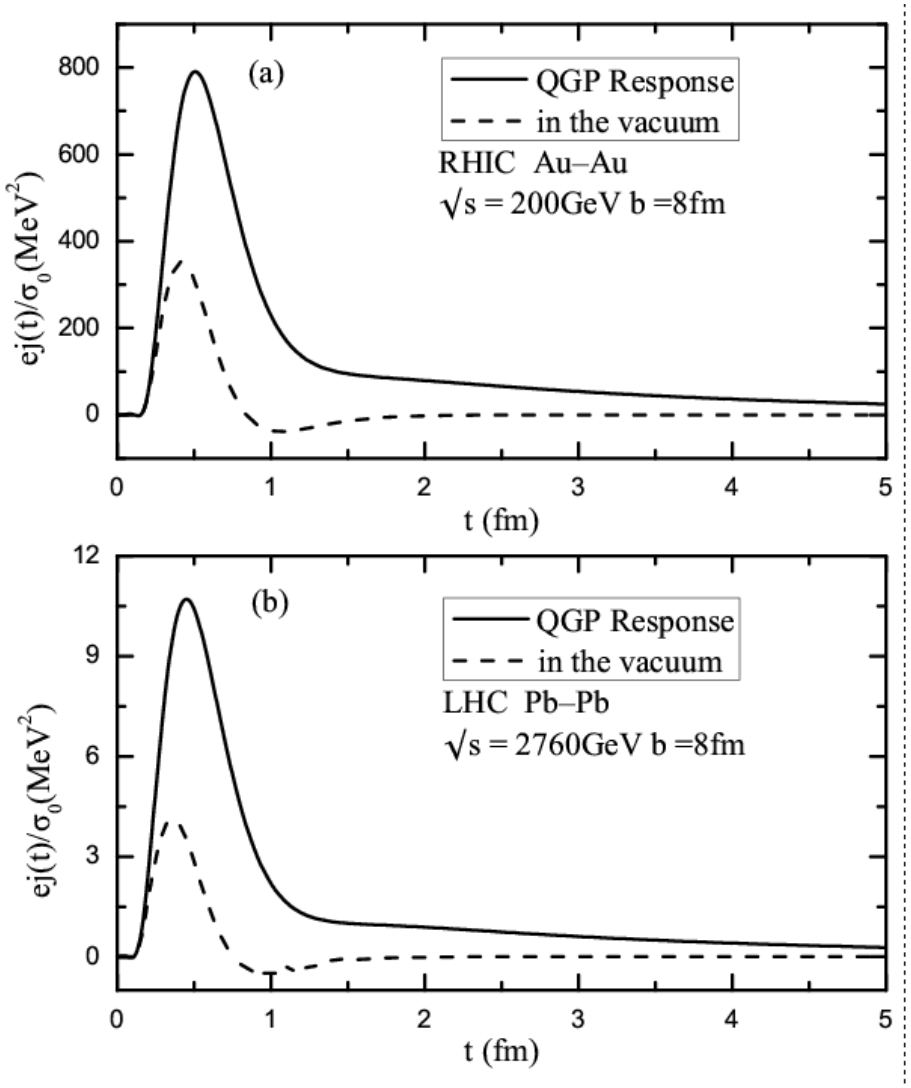

Maximum Chiral Electromagnetic Current (CEC) on energy and impact parameter

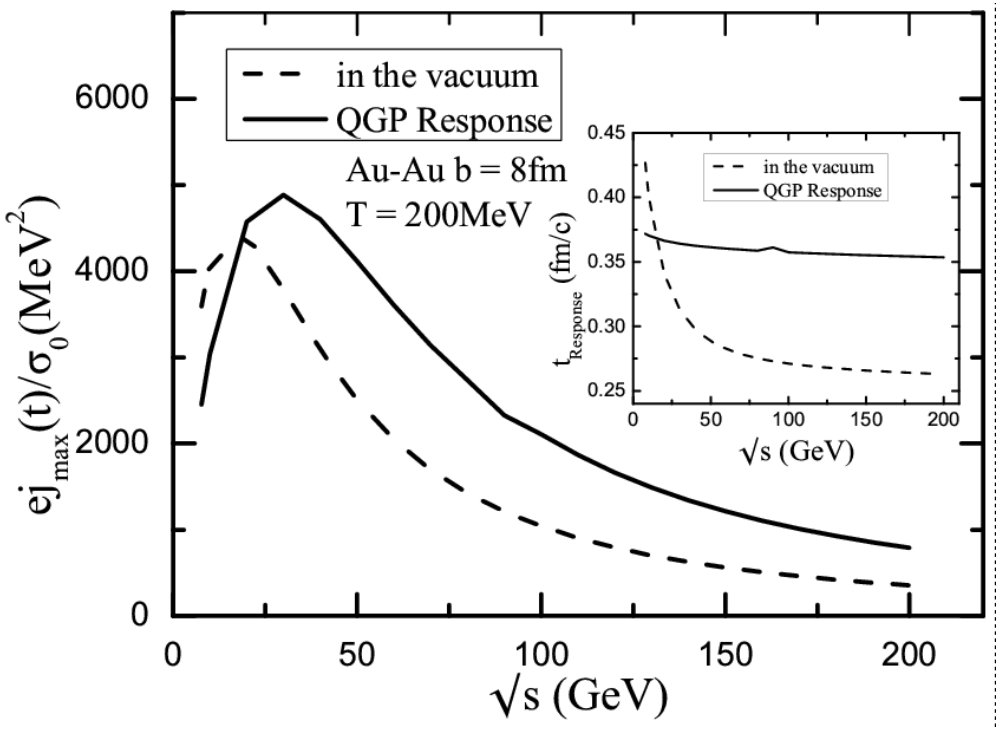

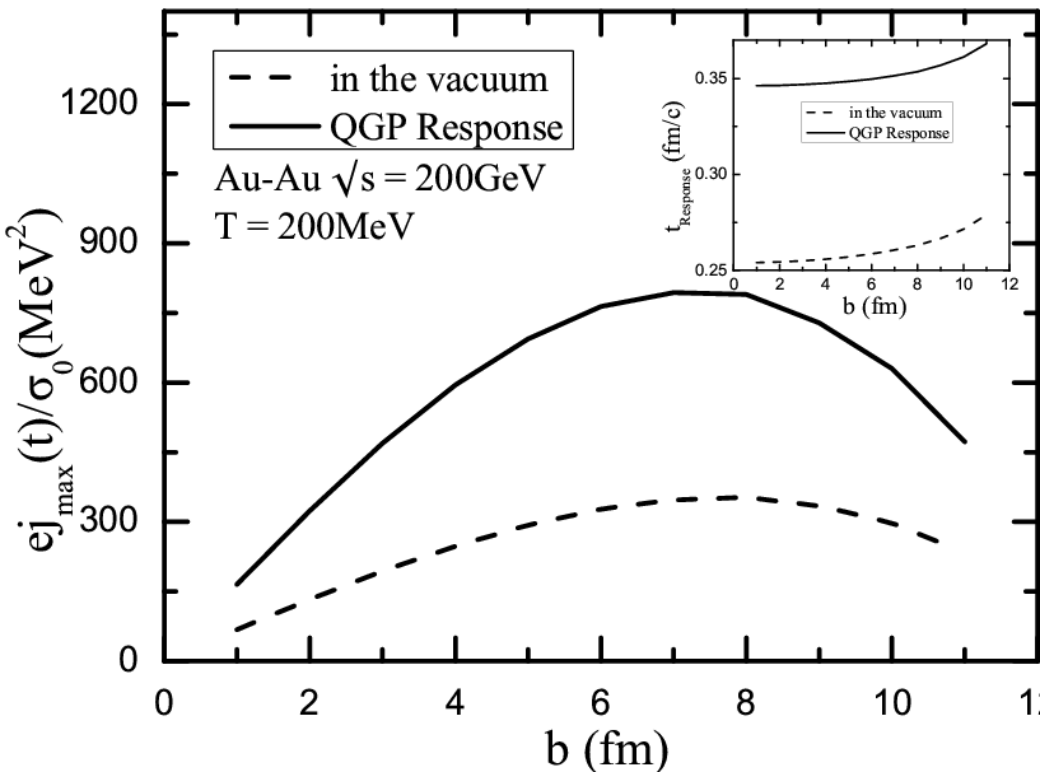

D. She, S. -Q. Feng, European Physical Journal A 54:48 (2018)

Chiral electromagnetic charge with different centrality

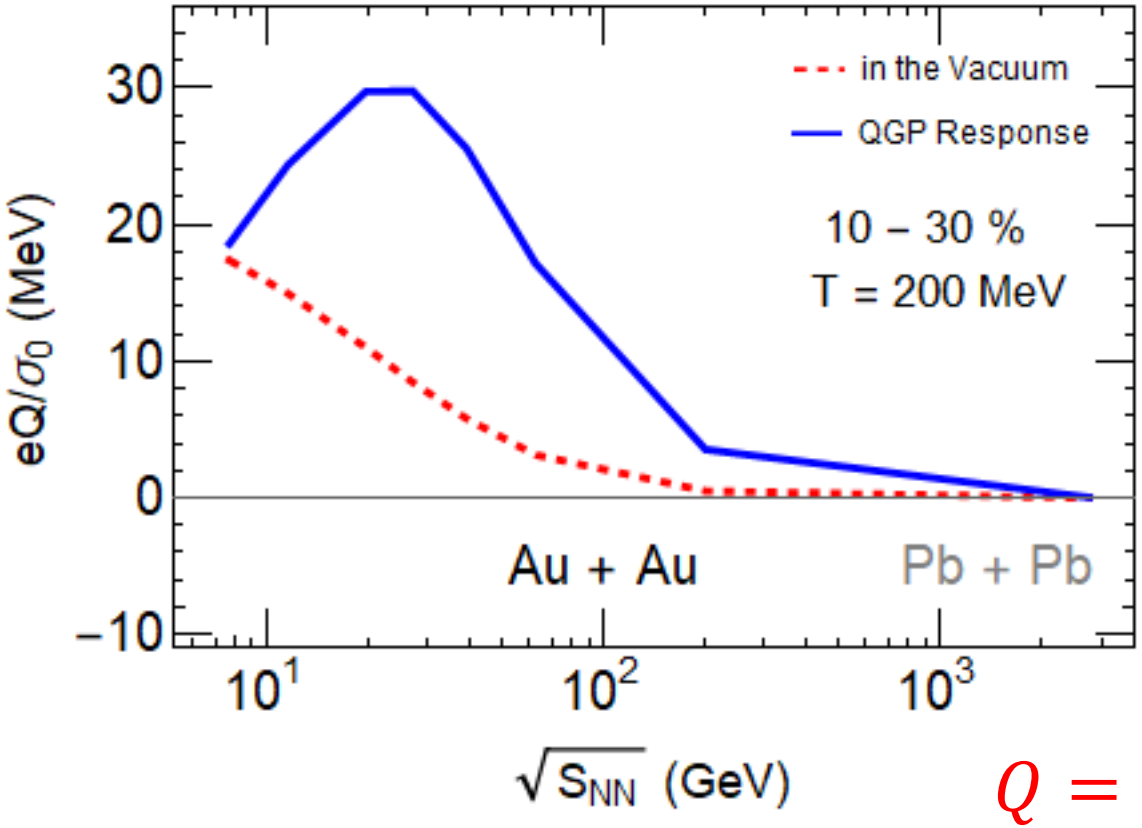

$$Q = \int j dt$$

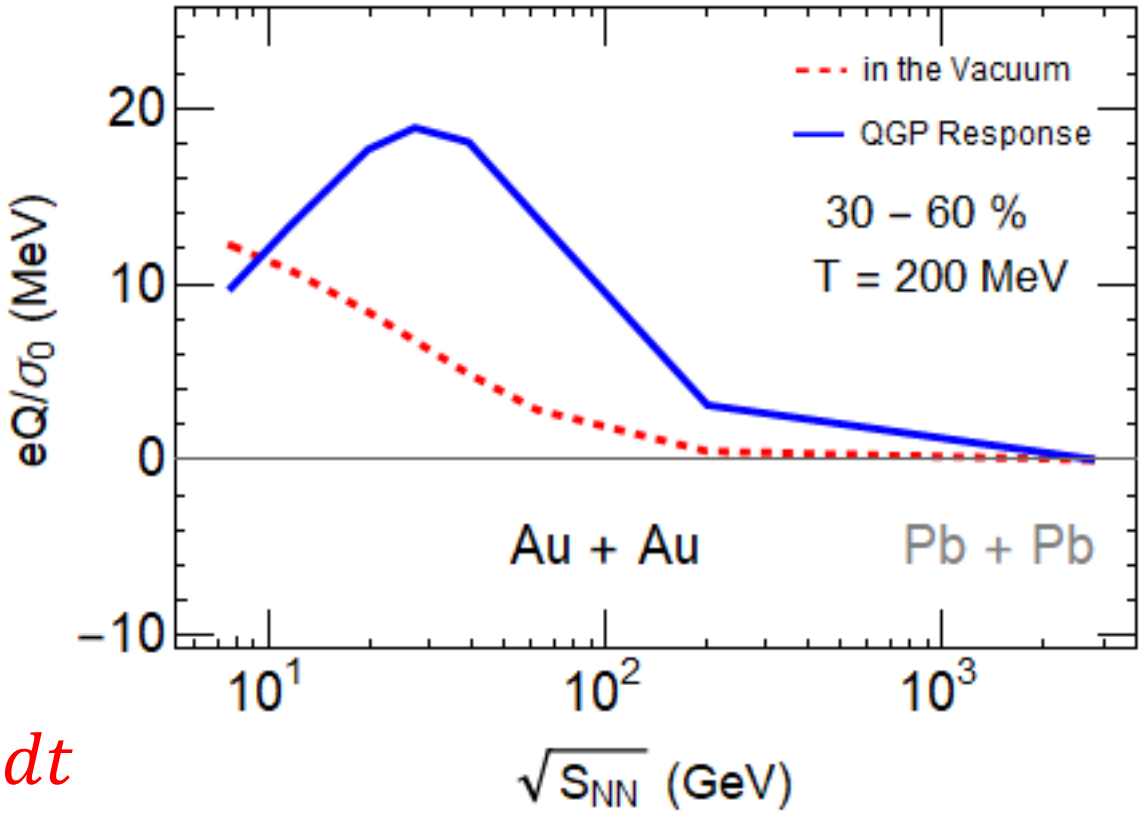

4. Charge Separation features in Relativistic HIC

Based on: S.-Q. Feng, X. Ai et al., Chinese Physics C 42 054102 (2018)

2019弦论、场论与宇宙学相专题研讨会，宜昌， November 22-25, 2019

CME Signal From Exp.

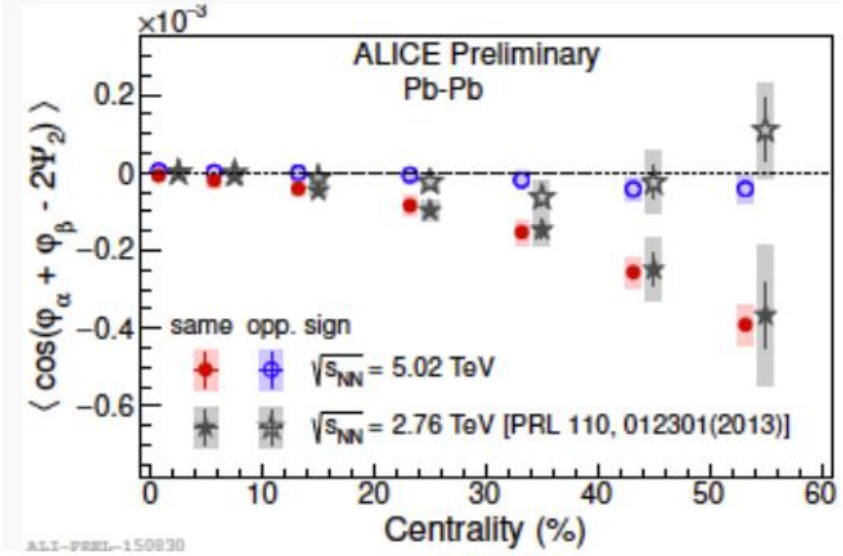

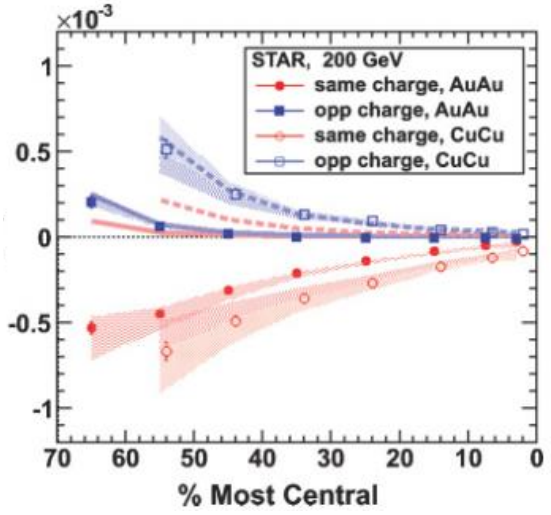

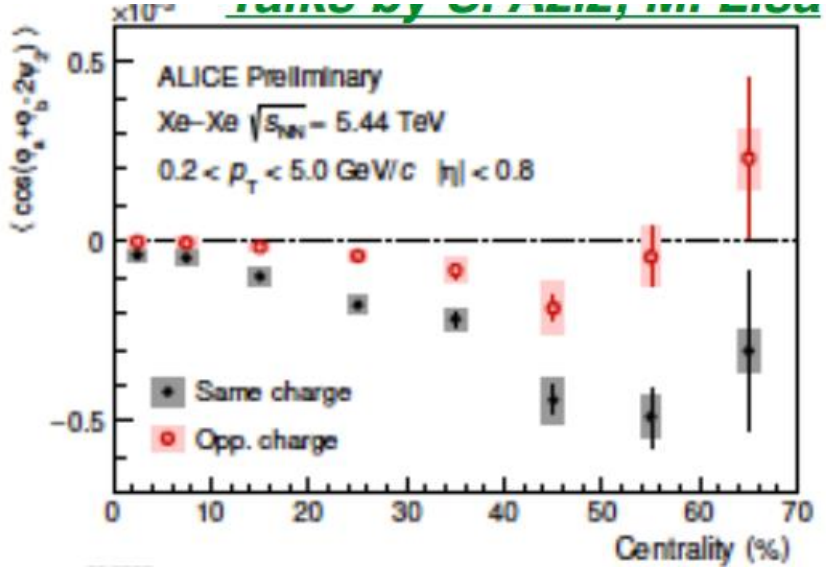

- *improving methods for background removal/suppression*
- *crucial to understand/reconcile different observables*
- *current RHIC results are hard to explain as pure background*
- *RHIC vs LHC important test for theoretical interpretations*
- *system scan would be useful too*
- *putting upper limit with confidence level would be very useful*

Calculate the charge separations between both sides of reaction plane

$$\langle \Delta_{\pm}^2 \rangle = 2\kappa\alpha_S \left[\sum_f q_f^2\right]^2 \int_{V_\perp} d^2x_\perp \left[\left(\xi_-(x_\perp)\right)^2 + \left(\xi_+(x_\perp)\right)^2\right] \int d\eta \int_{\tau_i}^{\tau_f} d\tau\, \tau [eB(\tau,\eta,x_\perp)]^2$$

$$\langle \Delta_+\Delta_- \rangle = -4\kappa\alpha_S \left[\sum_f q_f^2\right]^2 \int_{V_\perp} d^2x_\perp \xi_-(x_\perp)\xi_+(x_\perp) \int d\eta \int_{\tau_i}^{\tau_f} d\tau\, \tau [eB(\tau,\eta,x_\perp)]^2$$

$$\xi_\pm(x_\perp) = \exp\left(-\left|y_\pm(x) - y\right|/\lambda\right)$$

$$y_+(x) = -y_-(x) = \begin{cases} \sqrt{R^2 - (x - b/2)^2} & -R + b/2 \leqslant x \leqslant 0, \\ \sqrt{R^2 - (x + b/2)^2} & 0 \leqslant x \leqslant R - b/2, \end{cases}$$

The Chiral Magnetic Effect is a near the surface effect

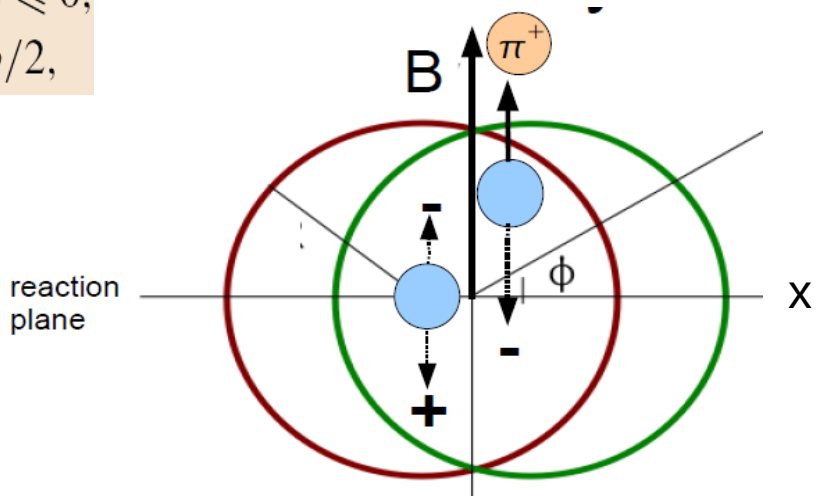

Calculate the charge separations between both sides of reaction plane

$$a_{++} = a_{--} = \frac{1}{N_+^2}\frac{\pi^2}{16}\langle \Delta_\pm^2 \rangle,$$

$$a_{+-} = a_{-+} = \frac{1}{N_+ N_-}\frac{\pi^2}{16}\langle \Delta_+ \Delta_- \rangle$$

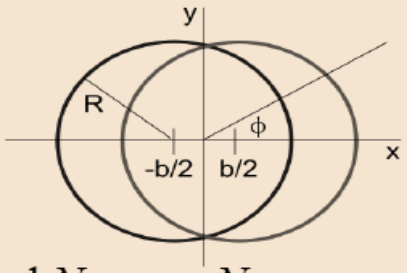

ϕ : angle between particle and reaction plane

$$\frac{\mathrm{d}N_\pm}{\mathrm{d}\phi} = \frac{N_\pm}{2\pi} + a_\pm \sin\phi + v_2 \cos 2\phi + \ldots.$$

Average over many equivalent events
(to cancel statistical fluctuations) can give us

$\langle a_+^2 \rangle \sim \langle \Delta_+^2 \rangle$ Pref. emission positive on one side

$\langle a_-^2 \rangle \sim \langle \Delta_-^2 \rangle$ Pref. emission negative on one side

$\langle a_+ a_- \rangle \sim \langle \Delta_+ \Delta_- \rangle$ Correlations between positive on one and negative on other side

Beam-Energy Dependence of Charge Separation along the Magnetic Field in Au + Au Collisions at RHIC

three particle correlator γ, two particle correlator δ ,

$$\gamma \equiv \langle \cos(\phi_1 + \phi_2 - 2\Psi_{\mathrm{RP}}) \rangle = \kappa v_2 F - H,$$

$$\delta \equiv \langle \cos(\phi_1 - \phi_2) \rangle = F + H,$$

where, H and F represent signal from CME and background， F mainly comes from elliptic flow.

$$H^{\kappa} = \frac{\kappa v_2 \delta - \gamma}{1 + \kappa v_2}.$$

Star's (14) used: H_{SS} , H_{OS}

can subtract non-flow background

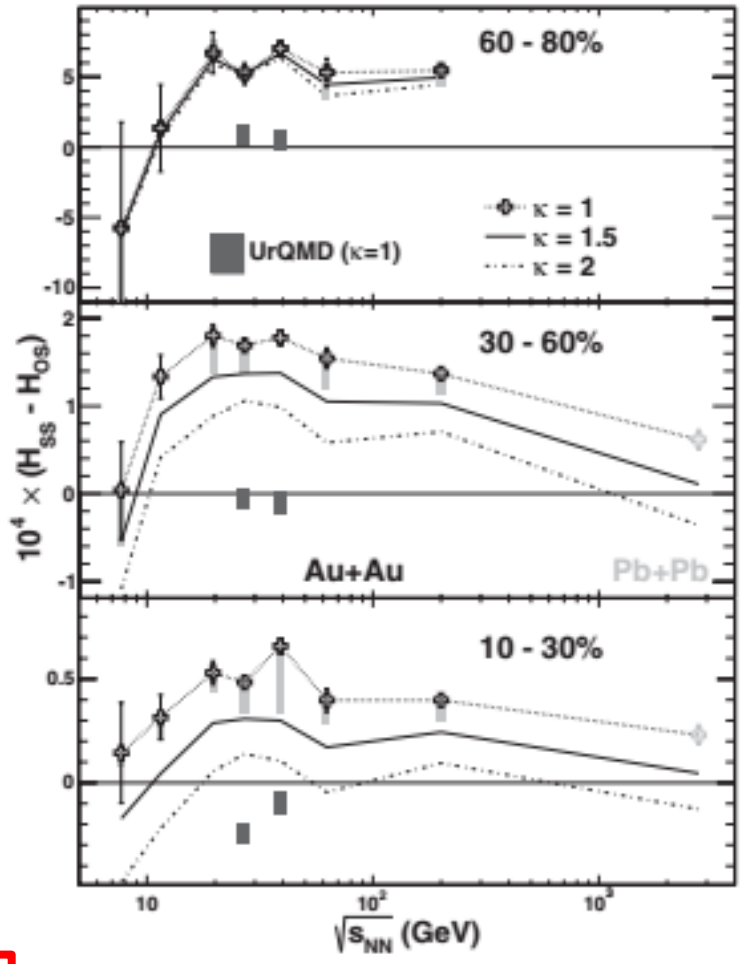

A. Bzdak, V. Koch, and J. Liao, Phys. Rev. C 83, 014905 (2011).
A. Bzdak, V. Koch, and J. Liao, Lect. Notes Phys. 871, 503 (2013)

Fit with BES experimental data

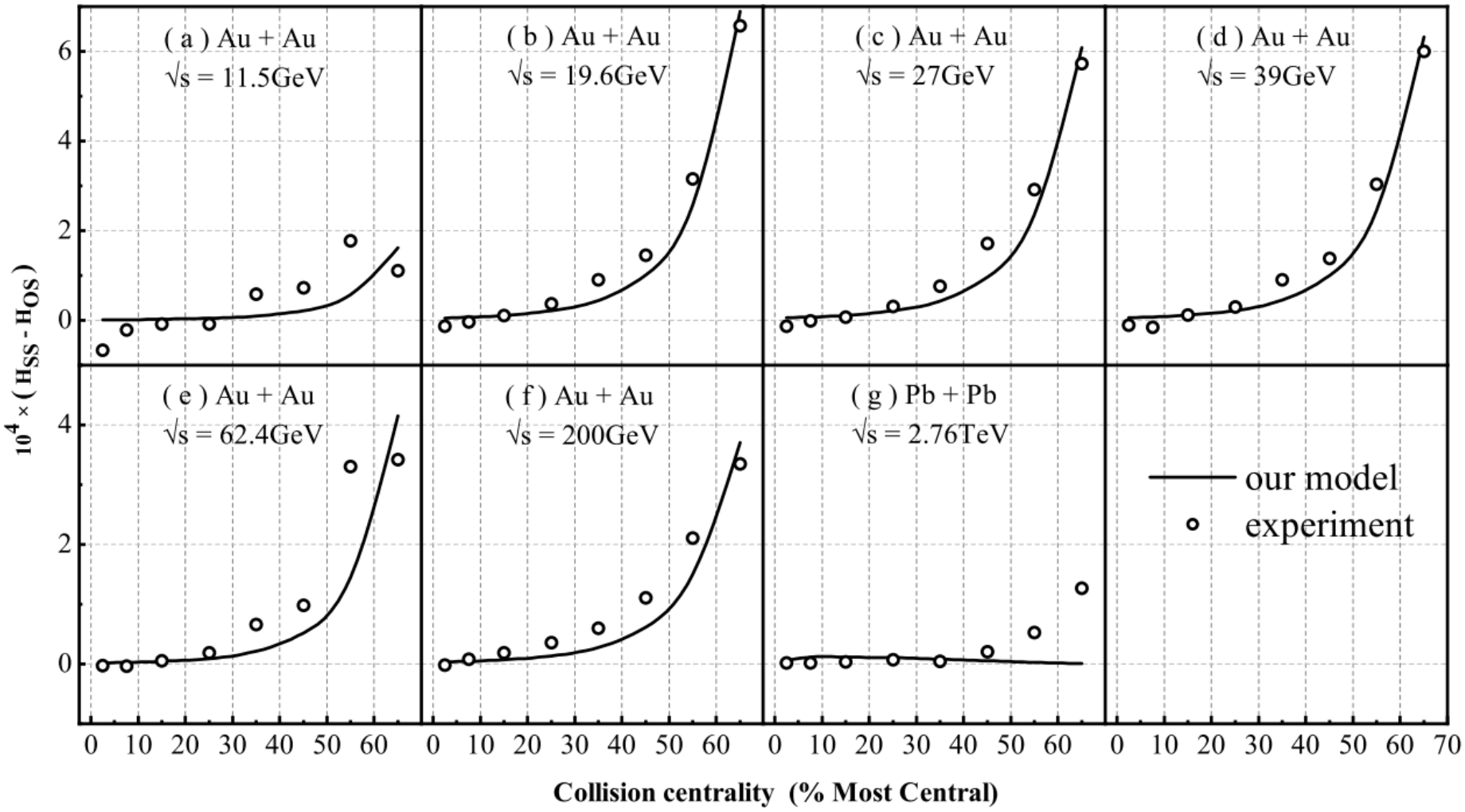

B. X. Chen, and S. Q. Feng, arXiv:1909.10836

Fit with experimental data

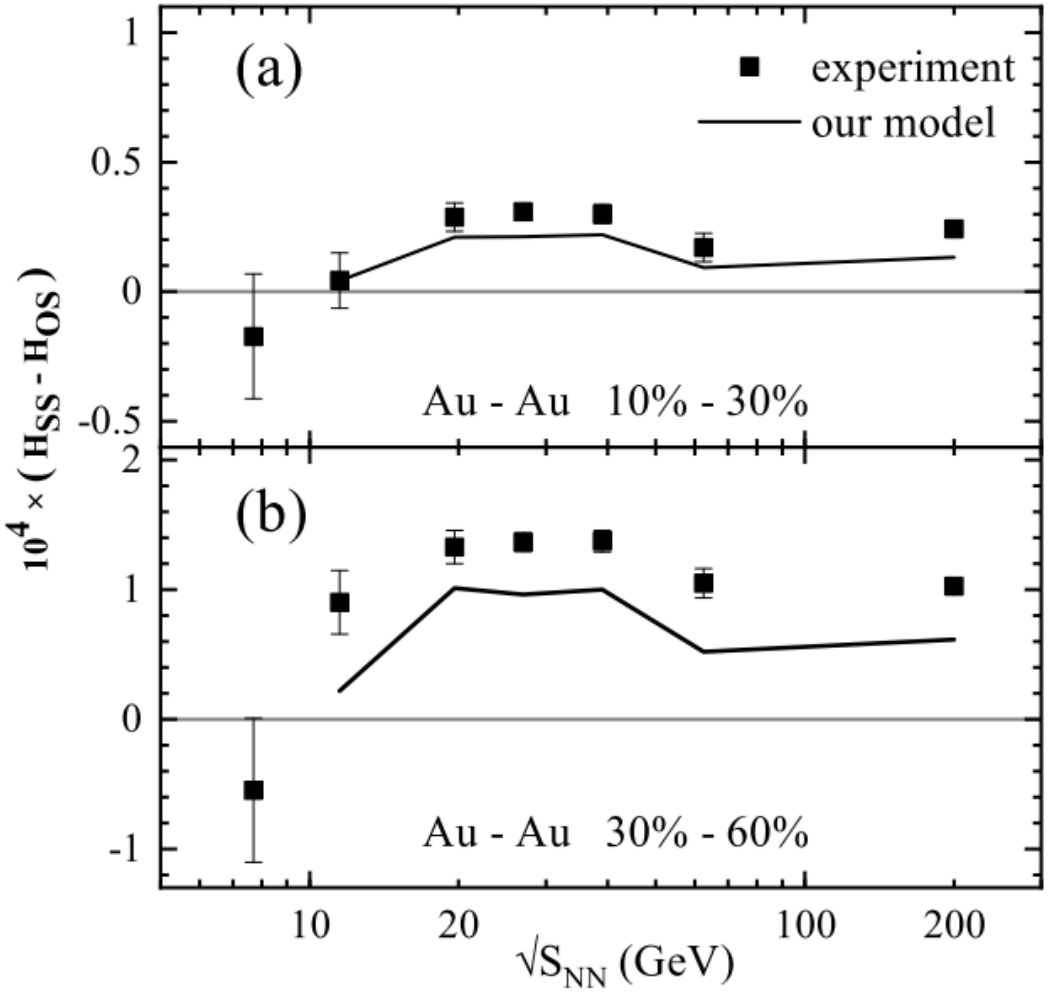

5. Magnetic field induced polarization difference between Λ and $\bar{\Lambda}$

Based on: Y. Guo, S. Shi, S.-Q. Feng, J. Liao, Physics Letters B 798, (2019) 134929

2019强论、场论与宇宙学相专题研讨会，宜昌， November 22-25, 2019

Extreme Vorticity & Magnetic Field

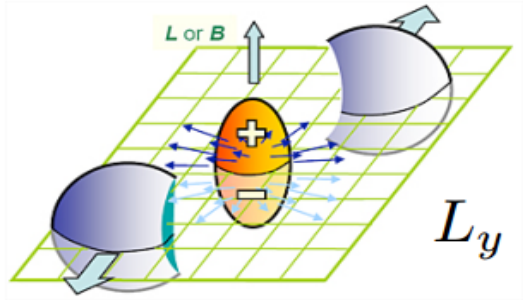

$$L_y = \frac{Ab\sqrt{s}}{2} \sim 10^{4\sim5}\hbar$$

$$eB \sim \gamma \frac{Z\alpha_{EM}}{R_A^2} \sim \text{few } \mathrm{m}_\pi^2$$

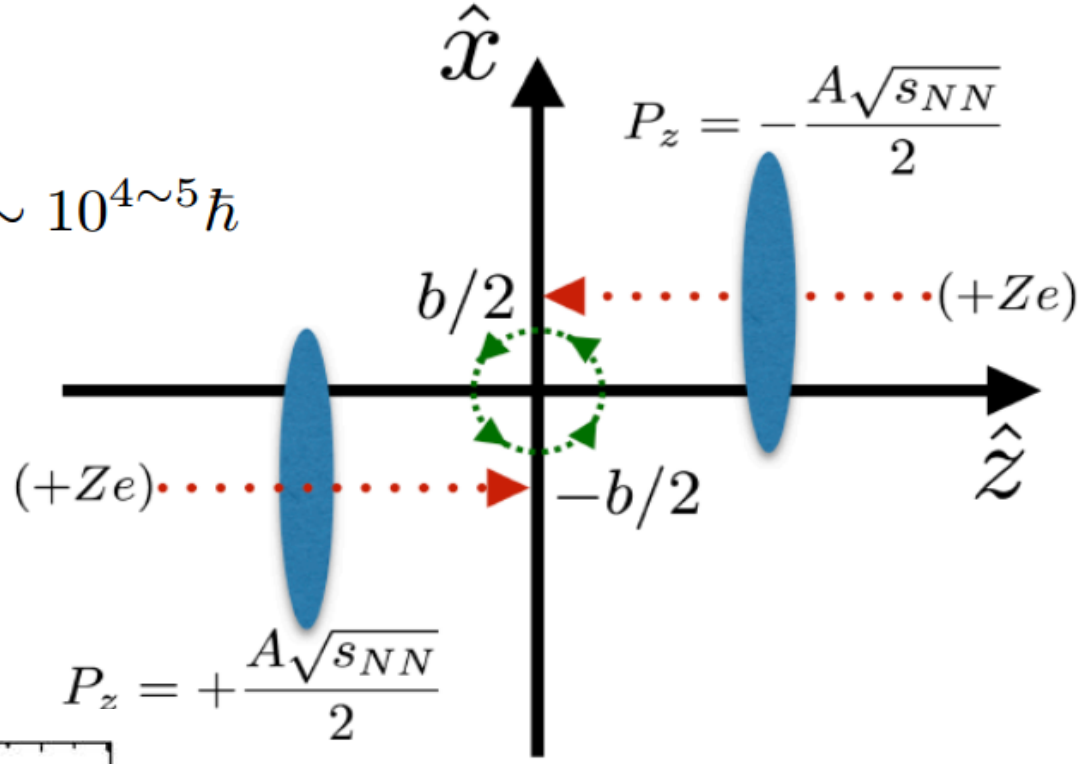

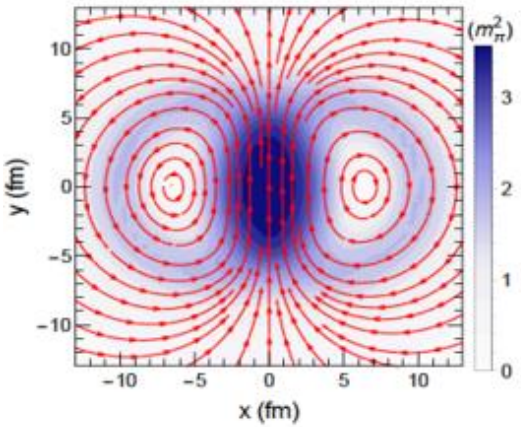

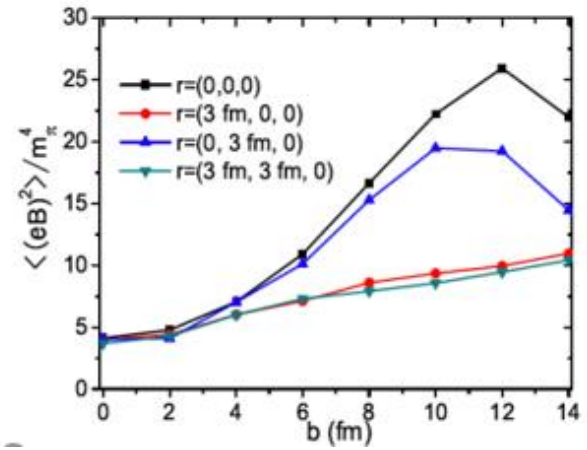

[Bloczynski, et al, arXiv:1209.6594[PLB]]

Magnetic field limits in polarization of Λ and $\bar{\Lambda}$

The recent discovery of a substantial global transverse polarization of Λ and $\bar{\Lambda}$ produced in peripheral heavy ion collisions has led to the conclusion that the quark gluon plasma is the "most vortical fluid" ever observed.

For this interpretation, it is of key importance that the polarization of Λ and $\bar{\Lambda}$ is the same within experimental errors, ruling out the presence of any sizeable magnetic field effect during the emission of the hyperons. This observation can be turned into an upper bound for the magnetic field strength at the time of hadronization of the quark-gluon plasma.

$$\Delta\mathcal{P} = \mathcal{P}_{\Lambda} - \mathcal{P}_{\bar{\Lambda}}$$

$$\mathcal{P}_i = \frac{N_i^{\uparrow} - N_i^{\downarrow}}{N_i^{\uparrow} + N_i^{\downarrow}}$$

where i denotes Λ and $\bar{\Lambda}$ and $\uparrow, \downarrow$ denotes particles with spin orientation parallel or anti-parallel to the global angular momentum vector of the colliding nuclear system.

Berndt Müller, Andreas Schäfer, PRD, 98: 071902 (2018)

Magnetic field limits in polarization of Λ and $\bar{\Lambda}$

The relative yield of thermally emitted hyperons with spin $\vec{s}$ is given by

$$N_i(\vec{s}) \propto \exp\left(\vec{s}\cdot\vec{\omega}/T_s + 2\mu_i\vec{s}\cdot\vec{B}/T_s\right),$$

where $\vec{\omega}$ denotes the vorticity of the matter, μ_i the magnetic moment of the (anti-)hyperon, $\vec{B}$ the magnetic field present at the moment of particle emission, and T_s is the temperature of the emitting source. Since the exponent is small compared to unity, it is sufficient to keep the linear term in the expansion of the exponentials

$$\mathcal{P}_\Lambda \approx \frac{\omega}{2T_s} + \frac{\mu_\Lambda B}{T_s},$$
$$\mathcal{P}_{\bar{\Lambda}} \approx \frac{\omega}{2T_s} - \frac{\mu_\Lambda B}{T_s},$$

where we used the fact that $\mu_{\bar{\Lambda}} = -\mu_\Lambda$ and ω and B denote the magnitude of the vorticity and magnetic field, respectively. Thus,

$$\Delta\mathcal{P} = \frac{2\mu_\Lambda B}{T_s}$$

Berndt Müller, Andreas Schäfer, PRD, 98: 071902 (2018)

Magnetic field limits in polarization of Λ and $\bar{\Lambda}$

$$\mathcal{P}_\Lambda = (0.277 \pm 0.040) \times 10^{-2},$$
$$\mathcal{P}_{\bar{\Lambda}} = (0.240 \pm 0.045) \times 10^{-2},$$

$$\Delta\mathcal{P} = (0.37 \pm 0.60) \times 10^{-3}$$

J. Adam et al. (STAR Collaboration), PRC, 98, 014910 (2018)

It is useful to consider the implications of the bound on the late-time magnetic field on the time integrated magnetic field $\tau_B e\bar{B}$ which governs the observable size of the chiral magnetic effect. Assumed an exponential decay of the magnetic field $B(t)= B_0 \exp(-t/\tau_B)$ with $eB_0 \approx 0.5 m_\pi^2$. The lifetime of the quark-gluon plasma in a 200 GeV Au - Au collision is $t_s \approx 5$ fm/c. Using the just derived limit $eB(t_s) < 0.0027\ m_\pi^2$ on the magnetic field at hadronization, we then obtain

$$\tau_B = t_s (B_0/B(t_s))^{-1} \approx 1 \text{ fm}/c$$

resulting in the estimate

$$\tau_B e\bar{B} \equiv \int_0^{t_s} eB(t)dt = \tau_B eB_0 < 0.25 \text{ fm}^{-1} \approx 50 \text{ MeV}$$

Berndt Müller, Andreas Schäfer, PRD, 98: 071902 (2018)

Polarization from Vorticity and Magnetic Field

In local equilibrium system, the ensemble-averaged spin polarization vector of the produced Λ and $\bar{\Lambda}$, with the existence of vorticity and magnetic field

$$S^{\mu} = -\frac{1}{8m}\epsilon^{\mu\nu\rho\sigma}p_{\nu}[\varpi_{\rho\sigma} \mp 2(eF_{\rho\sigma})\mu_{\Lambda}/T_{f}]$$

" - " for Λ, " + " for $\bar{\Lambda}$.

Polarization from vorticity

Polarization from magnetic field

The vorticity is $\varpi_{\mu\nu} = \frac{1}{2}(\partial_{\nu}\beta_{\mu} - \partial_{\mu}\beta_{\nu})$.

The absolute value of the $\Lambda(\bar{\Lambda})$ magnetic moment is $\mu_{\Lambda} = \frac{0.613}{2m_{N}}$.

The local temperature upon the particle's formation is $\epsilon \propto T^{4}$.

Follow the same step as in [1], after a Lorentz boost and average over all $\Lambda/\bar{\Lambda}$ produced at the hadronization stage of AMPT, we finally get the formula that can working on computer.

[1] H. Li, L. Pang, Q. Wang, and X. Xia, Phys. Rev. C 96, 054908 (2017).

Comparing with RHIC/STAR experimental results

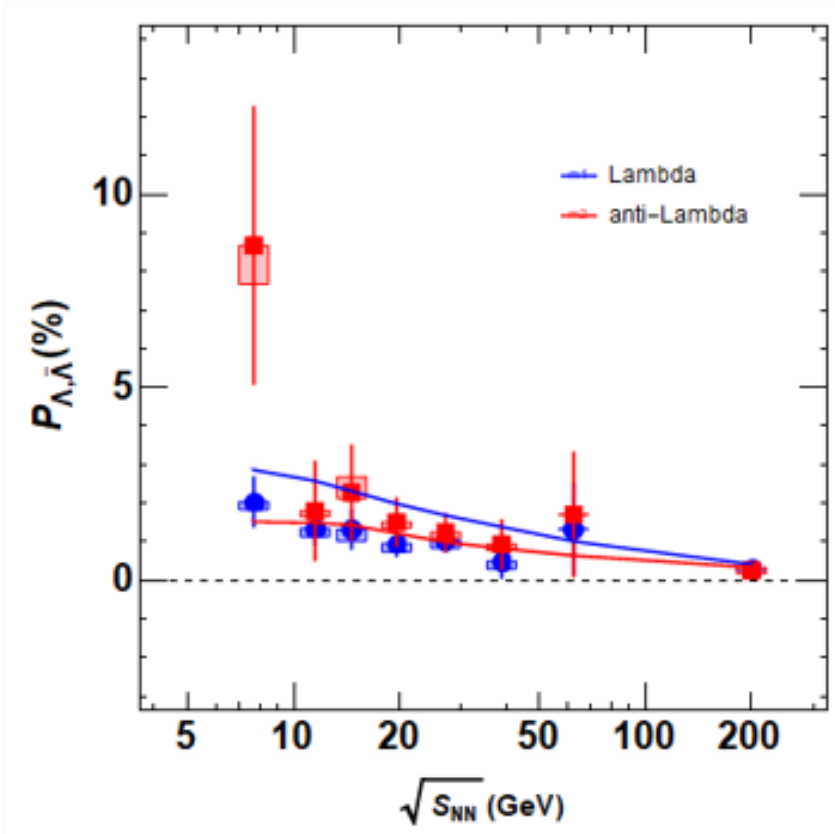

Polarization from vorticity only

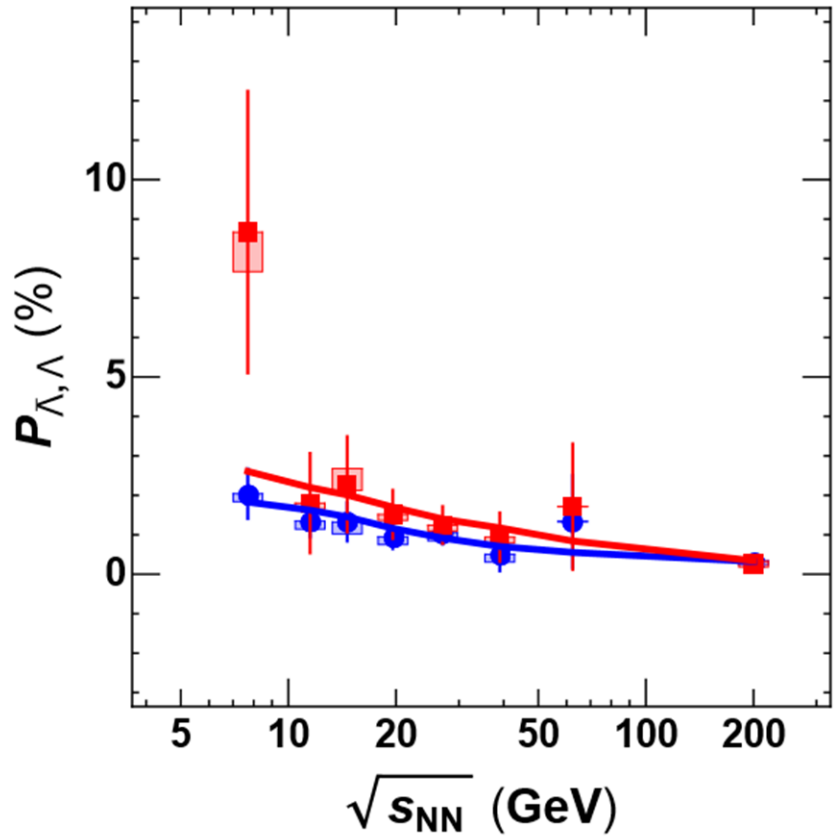

Polarization from both vorticity and magnetic field

L. Adamczyk, et al., STAR Collaboration, Nature 548 (2017) 62

How to Choose Magnetic Field Life Time Parameter t_B

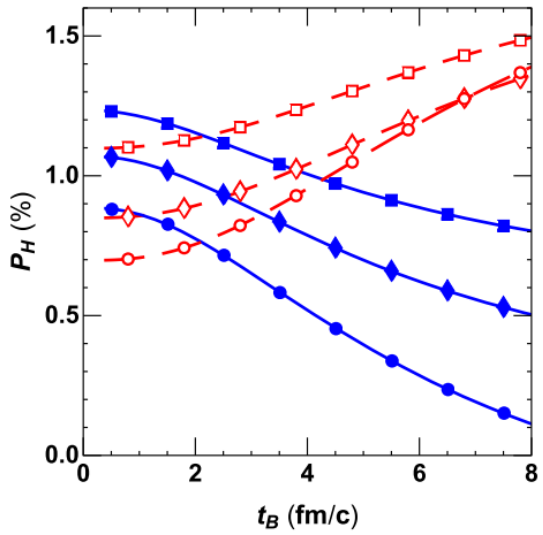

$H \rightarrow \Lambda$, blue solid curves with filled symbols

$H \rightarrow \bar{\Lambda}$, red dashed curves with open symbols

At beam energy 19.6GeV (square), 27GeV (diamond), 39 **GeV**(circle).

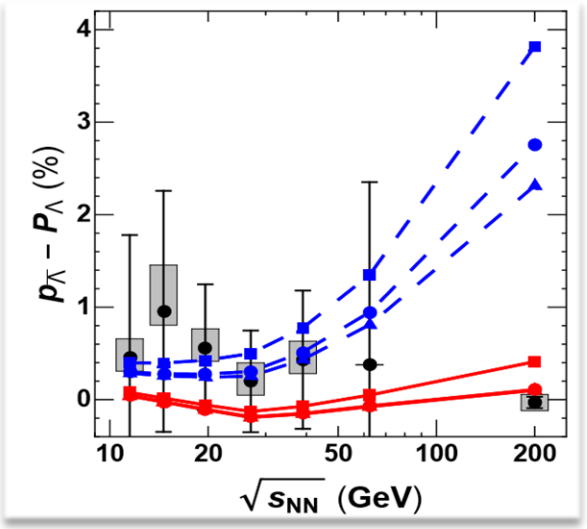

The difference $\Delta P = P_{\bar{\Lambda}} - P_{\Lambda}$ versus collision beam energy, for the type1 (square), type2 (diamond), type3 (circle) time dependence. The red solid curves are for $t_B = 1\ fm$ while the blue dashed curves are for $t_B = 4\ fm$. The black circles with error bars are STAR experimental data from **[1, 2]**.

Type 1: $F_B(t_b, t) = \frac{1}{1+(t-t_0)^2/t_B^2}$

Type 2: $F_B(t_b, t) = \frac{1}{[1+(t-t_0)^2/t_B^2]^{3/2}}$

Type 3: $F_B(t_b, t) = e^{-|t-t_0|/t_B}$

[1] L. Adamczyk, et al., STAR Collaboration, Nature 548 (2017) 62
[2] J. Adam, et al., STAR Collaboration, Phys. Rev. C 98 (2018) 014910,

Time Evolution of B-Field

Use phenomenology to constrain B-field lifetime:
t_B about 0.5~1 fm/c at RHIC

Type 1: $F_B(t_b, t) = \frac{1}{1+(t-t_0)^2/t_B^2}$

Type 2: $F_B(t_b, t) = \frac{1}{[1+(t-t_0)^2/t_B^2]^{3/2}}$

Type 3: $F_B(t_b, t) = e^{-|t-t_0|/t_B}$

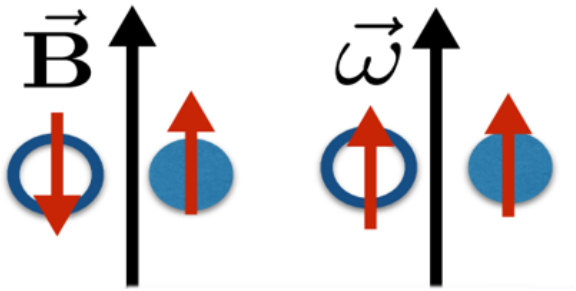

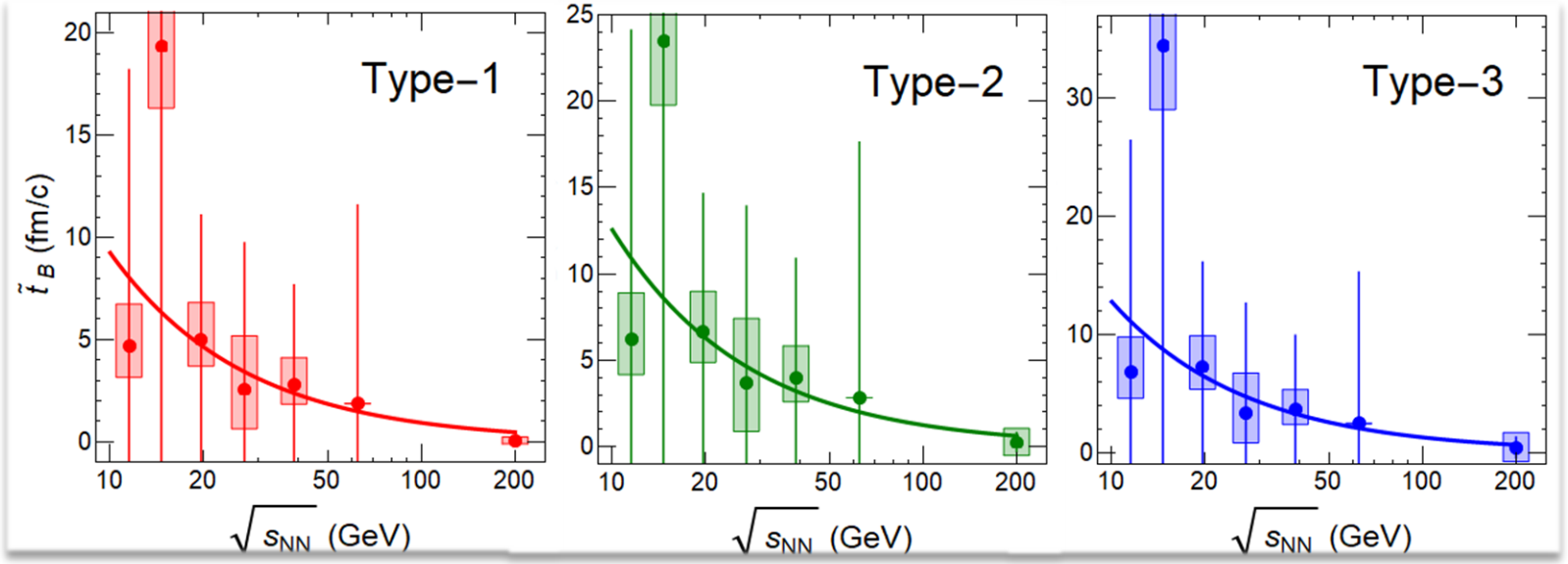

$$\tilde{t}_B = \frac{A}{\sqrt{s_{NN}}} \text{ with } A = 115 \pm 16 \text{ GeV} \cdot \text{fm/c}$$

Summary and Conclusions

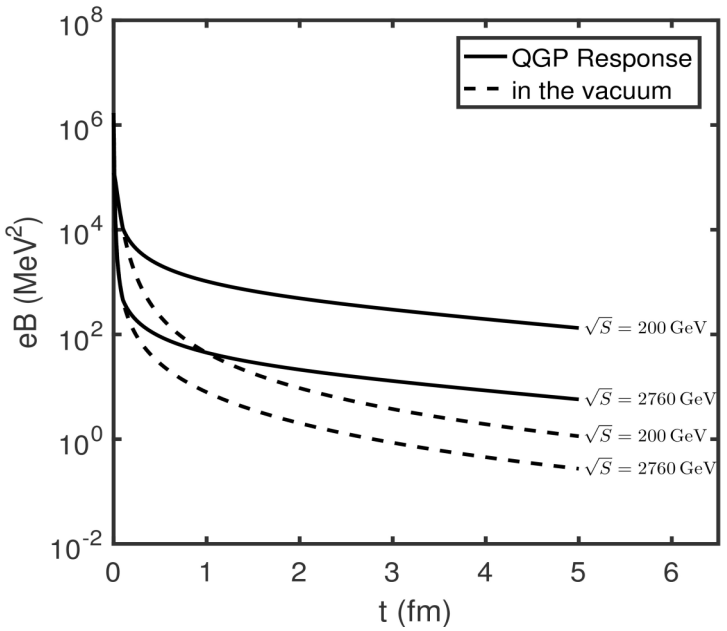

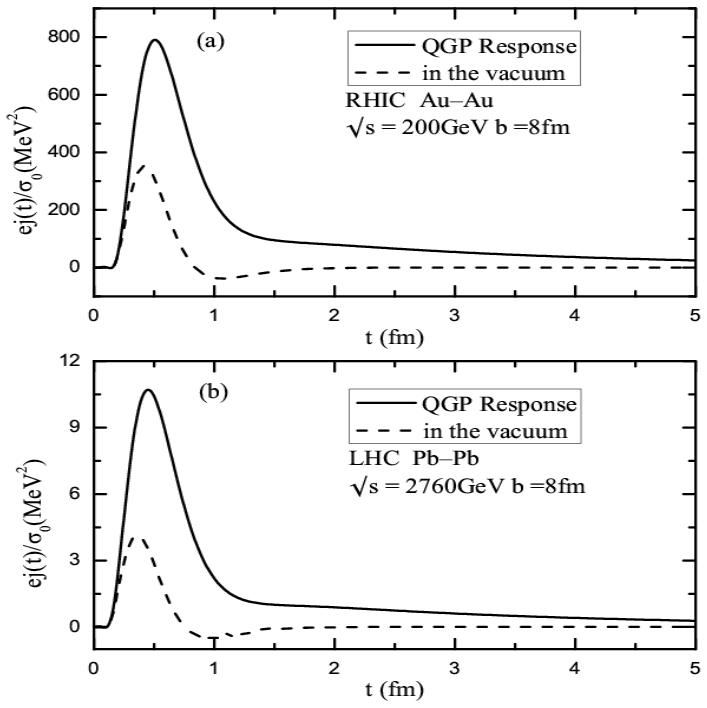

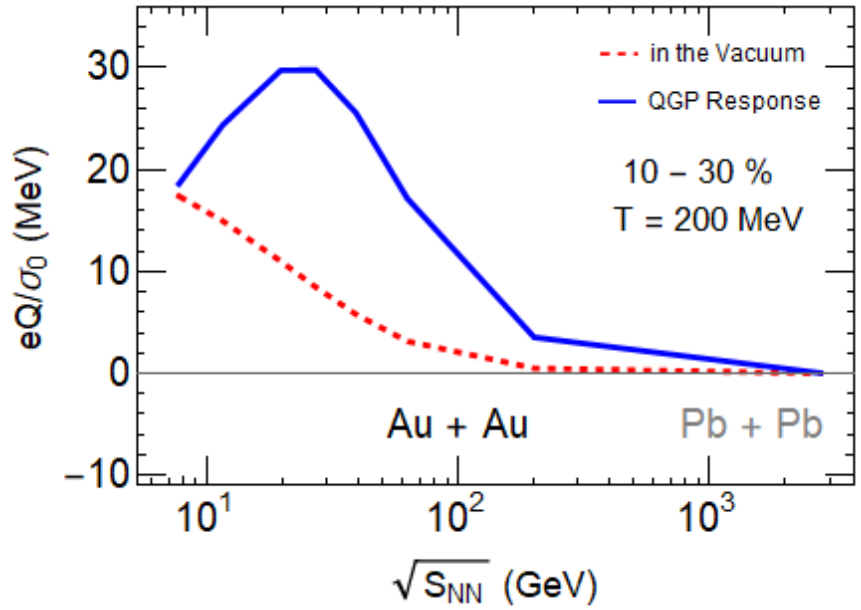

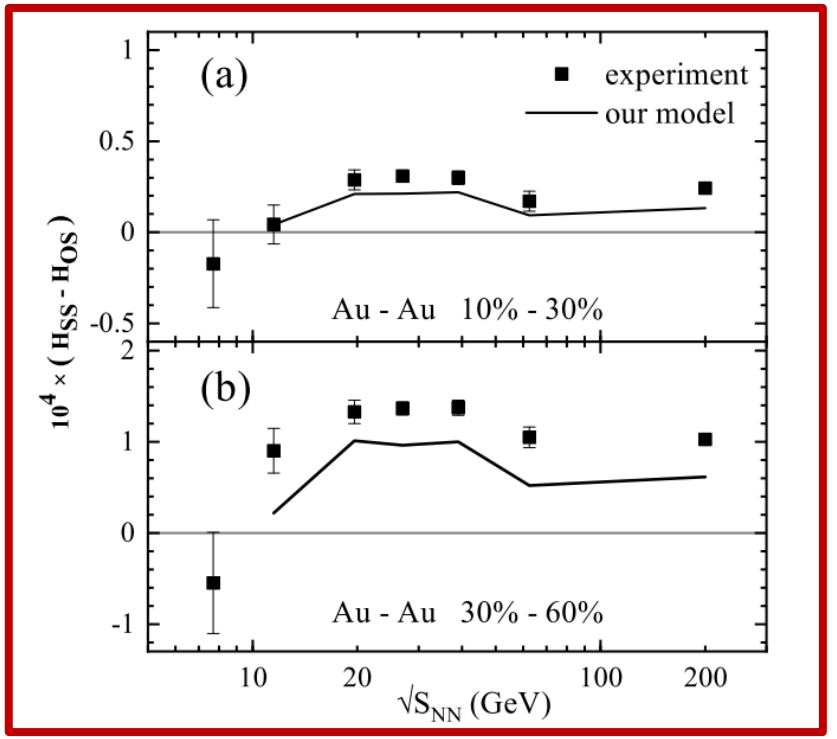

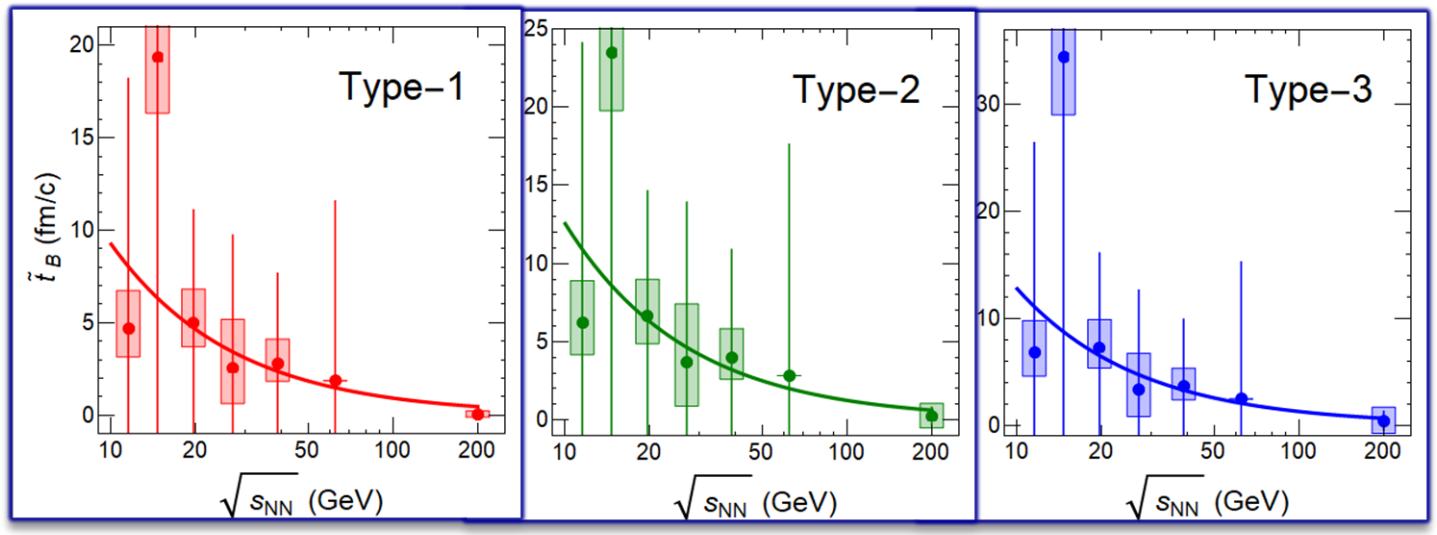

Thank your attentions